Selection of new drill sites using a Geographic Information System (GIS) at Los Azufres, Mexico

G.H. García-Estrada[1], A. López-Hernández[2,3] and J.L. Quijano León[1]
[1]Comisión Federal de Electricidad, Morelia, Mich., México, Correo: gerardo.garcía04@cfe.gob.mx.
[2]Facultad de Ingeniería Civil, Universidad Michoacana de San Nicolás de Hidalgo, Morelia, México.
[3]Posgrado en Ciencias de la Tierra, UACPyP – Universidad Nacional Autónoma de México, México, D.F.

Abstract

GIS technology is used to study the effects of distance between producing wells and superficial-thermal features and faults. It is used to interpret topographic lineaments and linear-resistivity interfaces at depth to identify hidden faults. Finally, a geothermal interpretation is conducted by applying a Multi-Criteria Evaluation Method (MCE) on a comprehensive data set, including geology, geophysics, and well production data. Visual comparisons of exploratory and drilling-data maps, with thermal discharge measured from wells, were used to select variables and data ranges that could be more directly associated with energy-production levels. Relative weights assigned by visual inspection are used to extend this knowledge to the whole exploration area. Criteria are compared to calculate a "geothermal index" representing the geothermal-production suitability for each cell into which the study area is divided. Considering the geometry of fault planes at depths from 700 to 2000 m below the surface, and a 250 m exclusion zone around productive wells, we choose areas from the normalized-geothermal index to propose new drill sites with different levels of risk, ranging from production (low risk) to exploration (high risk) boreholes.

Keywords: Los Azufres, drill-site location, Multi-Criteria Evaluation, decision making, Geographic Information Systems, Mexico.

Selección de nuevos sitios de perforación empleando un Sistema de Información Geográfica (SIG) en Los Azufres, México

Resumen

Se empleó la tecnología de Sistemas de Información Geográfica (SIG) para estudiar el efecto de la distancia de los pozos productores a las manifestaciones termales superficiales y a las fallas, y para interpretar los lineamientos topográficos y las interfaces lineales de resistividad a profundidad para identificar fallas ocultas. Finalmente, se realizó una interpretación geotérmica aplicando un Método Multi-Criterio de Evaluación (MCE) a un conjunto completo de datos que incluye geología, geofísica y datos de producción de pozos. Se utilizó una comparación visual de mapas de datos de exploración y perforación con descargas térmicas medidas en pozos, a fin de seleccionar variables y rangos de datos que podrían asociarse más directamente con niveles de producción de energía. Se usaron pesos relativos asignados por inspección visual para extender este conocimiento al total del área de exploración. Se compararon diferentes criterios para calcular un 'índice geotérmico' que representa la producción geotérmica potencial de cada celda en las que se dividió el área estudiada. Tomando en cuenta la geometría de los planos de fallas a profundidades de 700 a 2000 m, así como un zona de exclusión de 250 m alrededor de los pozos productores, se determinaron áreas de índices geotérmicos normalizados para proponer nuevos sitios de perforación con diferentes niveles de riesgo, que van de pozos productores (riesgo bajo) a exploratorios (riesgo alto).

Palabras clave: Los Azufres, localización de sitios de perforación, Evaluación Multi-Criterio, toma de decisiones, Sistemas de Información Geográfica, México.

Introduction

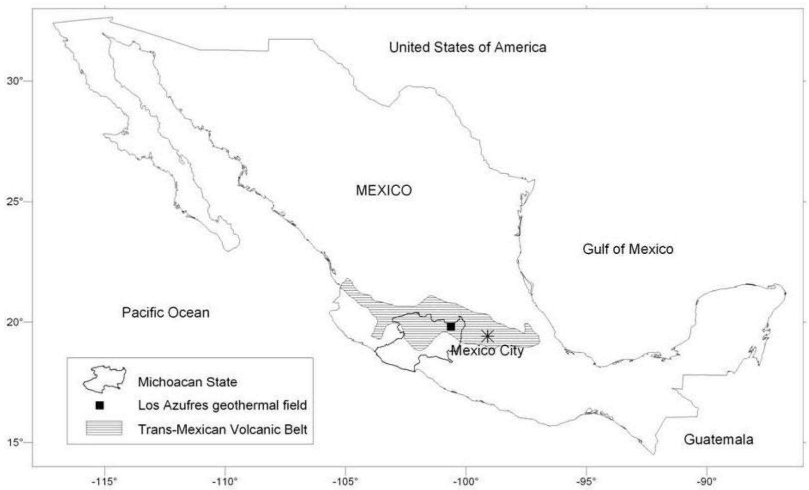

Fig. 1. Location of Los Azufres.

Los Azufres is the second largest geothermal field in Mexico, with a total installed capacity of 188 MW. It is located in the State of Michoacan, 200 km to the west of Mexico City (Fig. 1). A description of the geological setting is presented by Huitrón *et al.* (1991) and López (1991b). Increasing electricity generation in the last years makes necessary the location of new drill sites for replacing exhausted wells or to open new exploitation areas. After 20 years of exploitation a large amount of reservoir data has been accumulated while surface exploration studies still continue.

The conceptual model of the Los Azufres field postulates that there are two main up flow sectors, one in the north (Marítaro) and one to the south (Tejamaniles) (Fig. 2), separated at shallow depth (< 600 meters) by a relatively impervious rock (Agua Fría rhyolite). Both zones behave like a continuous reservoir at higher depth. Under natural (pre-exploitation) conditions, water flow at depth occurred from E to W but at present anomalous pressure gradients originated by the exploitation make injected fluid to move at production depth mainly from W to E (Residencia de Los Azufres, 1996).

The magma heat source has not been identified. Its location has been postulated under the central western sector where the youngest volcanic events, consisting of rhyolitic domes, are emplaced, but electric resistivity and temperatures at depth discourage that interpretation. The location of the highest stabilized temperatures, measured in low permeability rocks, to the east of the field suggest that the heat source can be a cooling magma body associated with the San Andres dacite dome that forms the maximum topographic prominence to the SE of Los Azufres (García-Estrada *et al.*, 2001). At depths over 2000 m the fluids up flow occurs trough a combination of NW-SE and N-S faults. From 2000 m depth to the surface hydrothermal activity is related to E-W faults. At a local scale flow through N-S and NE-SW fractures is important at shallow depths.

While our understanding of the field has increased, selection of new drill sites has turned more difficult, not only because the obvious locations have been drilled in the past, but also because to improve the criteria to locate new drill sites it is necessary to manage a huge data sets that overwhelm the human capacity of visual analysis and memory.

To overcome this obstacle and at the same time to make a more efficient data analysis, a practically complete data set of relevant geothermal data of each Mexican field, particularly at Los Azufres, was included in a Geographic Information System (García-Estrada and López-Hernández, 2003). In this way, an increased effort can be directed to research and development of new methods, ranging from map production to the development of more accurate conceptual models.

After the conclusion of the compilation stage, we started research in different subjects: a) the discovery or quantification of hidden relationship between geothermal variables on pre-existing data, b) the production of new geothermal results by data processing of digital maps recently acquired or re-interpreted, c) the development of methods assisted by the computer to systematize the comprehensive data interpretation required to locate new drill sites on the basis of present-day well established criteria, and d) the quantitative study of the geothermal significance of each variable to develop more accurate interpretation criteria, a task still in progress.

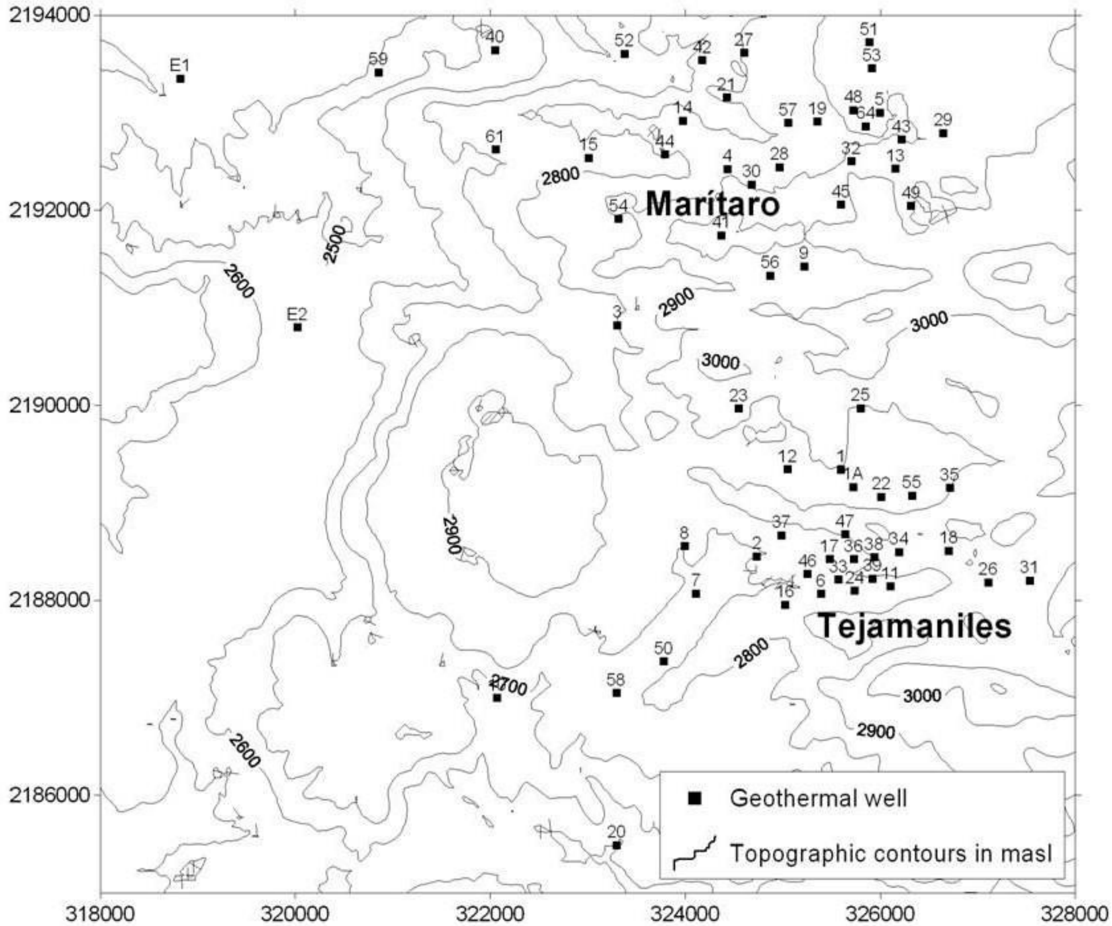

Fig. 2. General layout of the Los Azufres geothermal field, showing wells and topographic contours. UTM coordinates are in meters.

In this paper we present results from Los Azufres geothermal field related to the tasks described in the previous paragraph: 1) a quantitative analysis of the distance from production wells to surface thermal features and faults of different trends, 2) the production of new maps of lineaments useful to locate hidden faults, 3) the development and application of a Multi-Criteria Evaluation (MCE) method to make an integral interpretation of geothermal studies to locate new drill sites, and 4) the comparison of a geothermal suitability index based on pre-feasibility studies with that resulting from wells data, and their joint interpretation using weighted or non-weighted average procedures, an initial result of task d) described in the previous paragraph.

The development of the MCE method to locate drill sites is the main result of the paper. It is based mostly on the application of conventional intuitive criteria developed at Los Azufres along the past 20 years, in which this task has been conducted through the visual comparison of hard-copy maps. The modification of these criteria on the basis of statistical studies concerning the significance of each data layer or the identification of an optimum geothermal data set for selecting drill sites are part of task d) in progress. Results of statistical studies are of a more basic character; they concern the fundamentals of geothermal exploration and surpass the aim of this paper. Anyway, the MCE method implemented is adequate for the inclusion of different data sets or the modification of criteria for data integration required in the future.

2. Background

In this section we describe the conventional methods used to locate drill sites at Los Azufres, some unsolved questions and the previous usage of MCE methods at the geothermal division of the Comisión Federal de Electricidad (CFE).

2.1 Conventional procedure to select well drill sites

Around 70 deep wells have been drilled at Los Azufres by the CFE (Fig. 2). Most of them were located in places where, at the moment, it was considered that there was a chance to produce geothermal fluids. As expected, those wells located in areas far from the main thermal springs and faults had a higher risk to fail, so they had a partially exploratory character. The only two exceptions are wells E1 and E2 (slim wells), which were not adequate for fluid production even in the case of finding favorable conditions.

At present, around 42 wells are considered as ‘productive’ because they have adequate fluid enthalpies and flow rates to supply fluids to the power plants (Fig. 3). A list of water and steam production and mixture enthalpy is presented in Table 1.

There are other wells capable of discharging high enthalpy fluids but they are considered as non-productive because their thermodynamic conditions are not suitable for electricity generation under the prevailing production policies in the field. Some of those excluded wells could be considered as productive wells under less restrictive requirements prevailing in other Mexican geothermal fields. Fig. 4 shows a contour map of thermal discharge from productive wells.

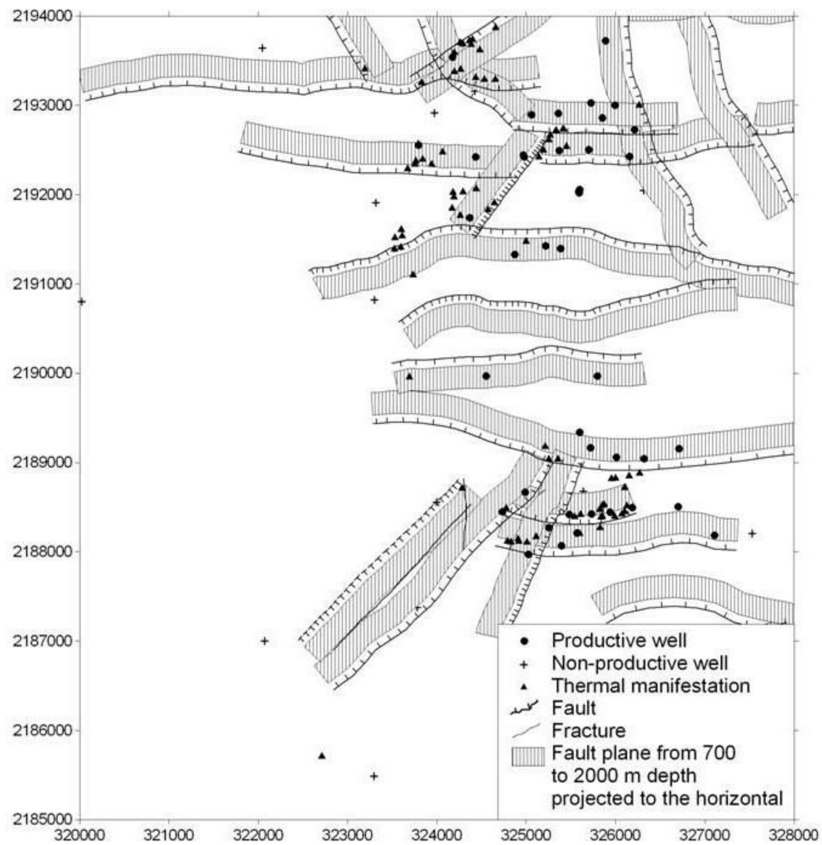

Fig. 3. Location of main geologic faults, superficial thermal manifestations and wells at Los Azufres. UTM coordinates are in meters.

Past experience in locating production wells at Los Azufres shows that the highest success rate is achieved when the intersection of E-W fault planes (Fig. 3) at depths from 700 to 2000 m below the surface are considered as the drill target. This criterion, along with the distance to surface manifestations and hydrothermal altered areas, serve as the best conventional indicators used to locate new drilling sites. Circulation losses during drilling, hydrothermal mineralogy, temperature and production data in nearby boreholes are also important (López, 1991a; Residencia de Los Azufres, 1996). Resistivity data at constant depths from 500 to 2000 m below the surface (Bigurra, 1995) are the most reliable geophysical tool, especially in areas far from previously drilled sites.

Well	X coordinate	Y coordinate	Height [masl]	Steam production [Ton/h]	Liquid production [Ton/h]	Mass flow [Ton/h]	Mixture Enthalpy [kJ/kg]	Thermal discharge MW	Steam quality %
1	325,597.02	2,189,340.00	2,863.60	23.9	8.8	32.6	2047	19	73
1A	325,721.61	2,189,164.00	2,875.39	34.7	2.1	36.8	2659	27	94
2	324,733.23	2,188,451.00	2,795.30	17.1	60.1	77.2	1182	25	22
4	324,432.89	2,192,423.00	2,871.36	30.8	23.6	54.3	1920	29	57
5	325,997.47	2,193,000.00	2,906.60	83.6	0.0	83.6	2775	64	100
6	325,393.01	2,188,066.00	2,822.15	37.0	0.0	37.0	2776	29	100
9	325,217.87	2,191,425.00	2,947.00	18.6	16.6	35.2	1829	18	53
9A	325,385.56	2,191,394.00	2,937.68	16.0	0.2	16.1	2753	12	99
9AD	325,385.56	2,191,394.00	2,937.68	22.4	0.0	22.4	2777	17	100
13	326,155.79	2,192,427.00	2,935.80	70.5	0.5	71.1	2765	55	99
16AD	325,026.40	2,187,972.00	2,831.58	20.3	11.6	31.9	2071	18	64
17	325,480.06	2,188,421.00	2,818.45	43.4	0.0	43.4	2769	33	100
18	326,704.02	2,188,507.00	2,953.63	47.3	0.3	47.6	2762	36	99
19	325,357.06	2,192,909.00	2,846.70	48.7	13.3	62.0	2348	40	79
22	326,008.84	2,189,061.00	2,863.43	102.4	64.2	166.6	2009	93	61
23	324,550.20	2,189,967.00	2,914.29	29.0	5.1	34.1	2472	23	85
25	325,796.05	2,189,970.00	2,895.09	15.2	8.8	23.9	2047	14	63
26	327,106.19	2,188,183.00	2,916.64	60.9	47.8	108.7	1880	57	56
28	324,968.72	2,192,443.00	2,852.04	68.9	9.5	78.4	2550	56	88
28A	325,368.36	2,192,493.00	2,859.92	17.4	5.1	22.6	2393	15	77
32	325,701.55	2,192,502.00	2,939.00	55.0	0.0	55.0	2783	43	100
33	325,569.52	2,188,212.00	2,838.70	60.8	0.0	60.8	2776	47	100
34	326,189.60	2,188,496.00	2,938.31	42.4	0.0	42.4	2772	33	100
35	326,711.91	2,189,155.00	2,877.15	48.4	0.0	48.4	2783	37	100
36	325,728.44	2,188,424.00	2,845.90	18.9	0.0	18.9	2774	15	100
37	324,988.08	2,188,667.00	2,845.24	34.2	0.0	34.2	2774	26	100
38	325,937.31	2,188,442.00	2,894.45	85.3	0.0	85.3	2774	66	100
41	324,369.97	2,191,742.00	3,011.00	13.1	0.0	13.1	2772	10	100
42	324,174.80	2,193,540.00	2,730.01	61.4	147.3	208.7	1378	80	29
43	326,215.75	2,192,726.00	2,898.80	51.7	6.5	58.2	2544	41	89
45	325,596.98	2,192,058.00	2,971.63	21.9	15.1	37.1	1989	20	59
46	325,253.64	2,188,270.00	2,817.10	63.0	0.0	63.0	2777	49	100
48	325,724.32	2,193,028.00	2,919.64	43.5	17.3	60.9	2202	37	72
51	325,888.73	2,193,723.00	2,915.02	32.3	19.2	51.5	2020	29	63
56R	324,873.27	2,191,331.00	2,927.68	16.9	0.7	17.5	2705	13	96
57	325,057.18	2,192,895.00	2,843.77	15.3	1.7	17.0	2581	12	90
62	326,320.00	2,189,044.00	2,867.00	89.6	87.7	177.3	1795	88	51
64	325,851.00	2,192,861.00	2,907.00	8.5	0.0	8.5	2772	7	100
65D	323,795.00	2,192,554.00	2,805.00	37.4	64.6	102.0	1503	43	37
66D	324,978.00	2,192,425.00	2,854.00	33.1	0.0	33.1	2777	26	100
67	325,594.00	2,192,023.00	2,973.00	19.7	0.1	19.8	2763	15	99
69D	325,586.00	2,192,037.00	2,972.00	67.2	0.0	67.2	2776	52	100

Table 1. Production, enthalpy, thermal discharge and steam quality of production wells in Los Azufres, year 2004 (only include wells actually integrated to the steam supply system).

Other methods have a more limited application. Gravity and magnetic studies conducted at Los Azufres (García, 1995) indicate that the field is located in a high density and high magnetic susceptibility block. Production wells are located near the flanks of the source body, but a detailed correlation with the production characteristics of wells has not been analyzed. Geochemistry of surface thermal features is seldom used because most manifestations are of acid type and an integral interpretation has not been done. On the other side, a few hot springs in the area are of carbonate type (of meteoric origin) and do not provide direct information on the reservoir (Tello, 1997; 2005).

Location of drill sites of a more exploratory nature (i.e., outside the current production area) depends to a higher degree on resistivity data, Schlumberger and Time Domain electromagnetic (Palma, 2003), and structural geology. Following these criteria, satisfactory results were obtained for exploratory wells 59, E1 and E2, but very disappointing results were obtained for wells 10, 20, 44 and 58, which were located as potential production wells. At the time they were drilled, more than ten years ago, these results were surprising because these wells had been located using the same criteria applied to locate the successful production wells drilled previously, i.e., near surface thermal features and to target minimum resistivity anomalies at depth.

In the case of wells 10, 20 and 58, later studies showed that the misinterpretation of minimum resistivity anomalies as direct indicators of reservoir conditions was the main error source. Now it is know that at Los

Azufres low but not minimum values are the best geothermal targets. In the case of the well 44, the recent drilling of a successful directional well (65d) at the same pad, indicated that the low permeability found in the first well was the consequence of drilling errors and a failed estimation of the depth to intercept a fault (the short distance between those wells makes them appear overlapped in Fig. 2 and 3).

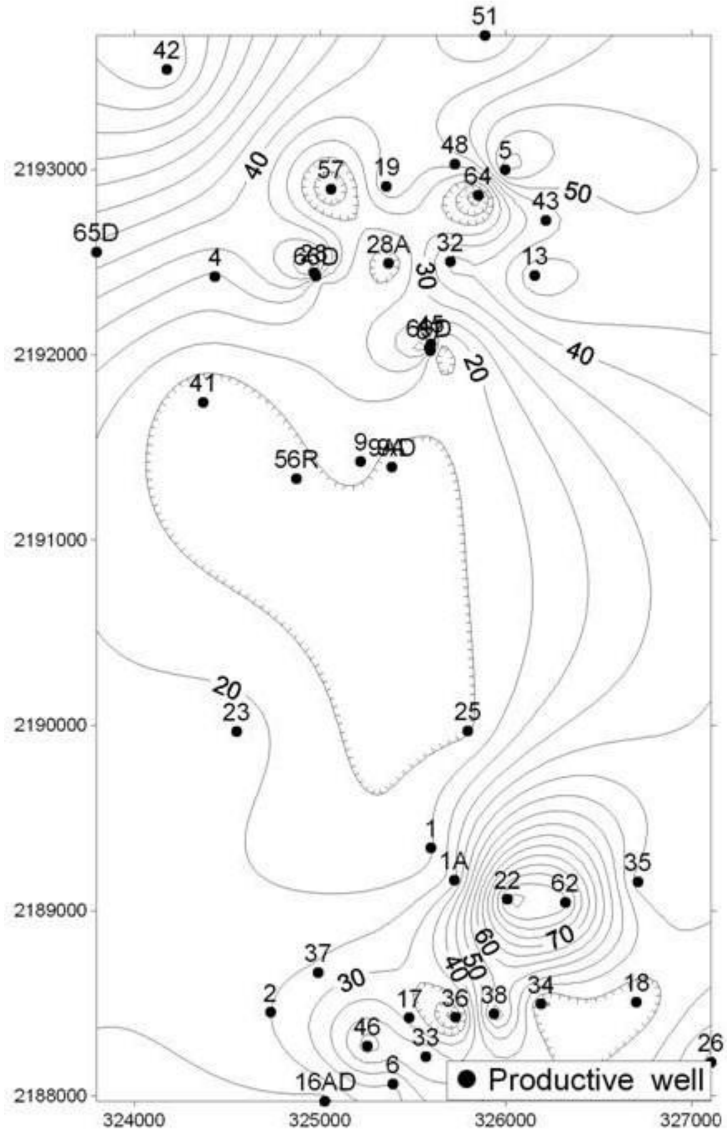

Fig. 4. Thermal discharge in MW in productive wells, calculated as the product of mixture flow rate and enthalpy. (Only wells actually integrated to the steam supply system as for August 2004 are shown. UTM coordinates in meters.)

After the preliminary selection of the best drill sites in plain view, the next step is the preparation of resistivity, temperature and mineralogy sections to confirm or reject the proposed sites. In all the cases, a subjective weighting of the encouraging and discouraging evidence is conducted by the interpreter, usually a geologist. Up to date, other data sources are not used because of the lack of clear-cut interpretation criteria and practical difficulties encountered in handling such large amounts of geothermal data. The MCE method described in this paper is aimed to provide the geologist a computer support for the stage of data integration in plain view.

In spite that Los Azufres is a well studied field, there are many basic subjects that are not well understood, in part due to the fact that some pre-feasibility studies were skipped or only partially applied (for example the measurement of the thermal discharge of surface manifestations). In this field it is difficult to measure the dip of faults at the surface because of the vegetation and the characteristics of the outcropping rocks. On the other side, the pattern of circulation losses in wells is complex, and the correlation of these with the fault traces at the surface has not been successful to determine the inclination of faults.

A constant 82° inclination for all the faults has been successfully used by CFE geologists to locate production wells at Los Azufres (López, 1991a). An inclination of 75° could be a better figure for a normal fault considering a theoretical homogeneous media model, but the 82° inclination has been accepted on the basis of measurements of topographic slopes and a few fault planes measured in the field.

A detailed structural geology study in progress (Rocha, 2007, personal communication) confirms the conclusions of previous studies conducted at different geothermal fields in Mexico, showing that the stress regime at the local scale can be quite different to that prevailing at a regional scale, and changes can occur at the scale of a few kilometers depending of the properties of the local rocks and the effect of recent magma intrusions. Fault dips around 75° were recently inferred for two sites on the basis of micro-structural measurements. New field data show a NE-SW offset on at least one E-W fault, suggesting the local reactivation of the NE-SW fault system. On the local scale, it was observed that some thermal manifestations are aligned over NE-SW and especially N-S trends. For our analysis we decided to use the conventionally accepted 82° constant inclination as long as specific data for each fault are not available.

Petrologic studies in wells usually identify abundant microscopic structures associated with faulting. On the other hand, circulation losses and thermal logs suggest that permeable zones underground are not restricted to faults mapped at the surface. We consider that an explanation in some cases is the existence of not previously identified superficial faults with orientations other than E-W. The existence of hidden faults at Los Azufres is suggested also by the local changes in the distribution of thermal features respective the dominant E-W regional trend, results of structural geology studies, unexpected patterns of circulation looses in wells and high production in wells not clearly associated with known faults.

2.2. Antecedents on Multi-Criteria Evaluation Method

We decided to follow a direct modeling approach for data integration because it is the conventional procedure applied at the CFE to locate new drilling sites. In this way we can profit from the geologist experience to assign a different significance for each geothermal study as a geothermal clue to locate drilling sites, and at the same time we promote the systematic application of the methodology assisted by the computer that we created. Methods based on inverse modeling could be developed only after the conclusion of the statistical studies in progress, because we consider that it is necessary to reach a better quantitative understanding of the information provided by each data source before attempting to automate some steps of data integration.

Multi-Criteria Evaluation methods are designed to make the joint evaluation of an area on the basis of different data sources (layers). They transform information corresponding to each data source to a numeric variable that reflects their suitability for a certain usage. Usually these methods use a weighted average (a linear combination) to obtain the resulting value. Ideally, weighting values should be based on calibration zones on which known results of the output (dependant) variable can be reproduced by means of an adequate selection of data weights. However, very often, as in the present study, the assignment of weighted values relies more on trial and error tests and the personal experience of the interpreter.

We consider that the use of a Multi-Criteria Evaluation method (MCE) is a good starting point because beside it does not constitutes a radical break with conventional interpretation practices, its application does not depend on the statistical treatments that we have just initiated, and so, the obtaining of results of practical interest in the short term is guaranteed. We assume that the data used for this study are relevant for drill site location, without a statistical demonstration, because it has been used successfully to locate drilling sites in the past 20 years. The quantification of the relative significance of each data layer and the definition of the minimum significant data set for this task, eliminating redundant layers, are the kind of technical concerns requiring a detailed statistical study.

The use of a MCE is a natural way to increase, step by step, the rigor used to conduct the joint interpretation of multiple geothermal data sets. Through the application of explicit criteria to evaluate each parameter, it provides a basis to develop methods with a better statistical support in the future. Finally, previous experience of the CFE personnel in the use of MCE procedures is also a fundamental reason to opt for this method.

Multi-Criteria Evaluation Methods were used at the CFE in early 1980’s as a preliminary task to select promising geothermal areas to be verified during field research for the First National Census of Thermal Manifestations in the country. Pre-existing Earth Sciences regional maps and photo-interpreted linear features and volcanic edifices on Landsat IV images, among other variables, were the raw data (López-Hernández *et al.*, 1981).

At that time, results were highly satisfactory in spite that the numeric procedure was applied without the aid of a computer. The studied area was divided using a regular square grid overlying the satellite image, and on each grid cell vertices a numeric value reflecting the density of linear features, volcanoes or the lithologic type were indicated. After normalizing the values of each variable, the user calculated a resultant number by means of a weighted linear combination of the partial qualification corresponding to each variable. Usually each weight was decided by the user on the basis of his or her experience and the known characteristics of the studied area.

It can appear that due to the subjectivity in the selection of weights, the MCE method has a very limited utility for the study of a particular area, and is completely useless to compare results from different geothermal projects. Those criticisms have certain justification but, on the contrary, we can argue that a MCE procedure has invaluable advantages that make advisable its application. The first one is that it makes necessary the explicit identification of the variables on which a conclusion will be dependant, and also that it requires explicit data combination criteria. Both conditions make the process more or less repeatable, with the advantage that it can permit the inclusion of new data and criteria according to the interpreter's experience. Those attributes of MCE explain the successful results obtained at CFE.

At a geothermal field scale, Prol-Ledesma (2000) used a GIS to predict the location of the most productive areas within the Los Azufres field using a MCE method. That study assigned a 'geothermal favorability index' based in apparent electric resistivities for AB/2 = 1000 m and the distance from geologic contacts, faults, fractures and thermal manifestations. Although many producing wells were left out the areas marked as favorable, none of the non-producing wells were included in them, so the 'low-risk' map was considered by that author as suitable for exploration well sitting.

Since the time that study was conducted to the present, new production wells (64, 65d, 66d, 67, 69d, 9AD, 1A, 28A, 9A, 19d) and an injection well (7A) have been drilled, and two more were repaired (29d, 53). However, the new drilling results are not adequate to test the conclusions of that paper because most wells were drilled in well known productive areas at a distance of no more than 500 m away from previously drilled wells. On the other side, figures in the cited paper have not the adequate size to make a detailed analysis. As a result of a visual scrutiny, we consider that the new drilling results are better represented by the geothermal favorability map of high-risk using a Fuzzy Logic model (Fig. 10 of the cited paper). Other methods illustrated in the same paper produce results so restrictive that do not classify adequately productive wells (either pre-existent at the time the study was conducted or recently drilled).

3. Methodology

For our study, the location of thermal springs at Los Azufres is based on maps elaborated before Global Positioning System (GPS) technology was available. Most coordinates were digitized using a tablet and hard copy maps elaborated 25 years ago. A new inventory of thermal manifestation locations using GPS is in progress as part of the structural geology research project in progress. Preliminary results were available for this study (Fig. 3).

Coordinates of most wells were determined by the CFE's field personnel using GPS technology; in a few cases, their location is based on digitizing coordinates from hard copy maps. Fault traces were digitized from geological maps with a scale 1:10,000 (López, 1991a) based on field work. Cartographic deformations and fault traces were corrected to fit the topographic slopes observed on shadow relief maps of a digital elevation model with a 10 x 10 pixel.

All this information was geo-referenced using the new Mexican cartographic standard Datum (ITRF 92) to include them in the GIS. In spite that some mapped features require further modification, this data set is the best and more reliable source available to make the study described in this paper.

3.1 Relation of production wells to thermal features and different fault trends

To study the importance of distance from production wells to superficial thermal features, or from production wells to faults of different trends, a simple distance analysis was conducted. What we did is to find the nearest neighbor for each one of the elements of the two sets, wells and thermal features, respectively. The 'production' or 'non-production' attribute of each well was used to classify the distance to the nearest thermal feature in two groups, and then the average minimum distance was calculated for each one.

In the case of faults we follow a similar approach but in that case the attribute 'trend' of each fault was used to form subgroups of minimum distance depending on the well type and the fault trend. Average trends of linear features are automatically calculated inside the system and the resulting data are grouped into classes according the user defined azimuth intervals. We defined four classes of fault trends that we considered relevant for Los Azufres: N-S, E-W, NW-SE, and NE-SW. As the final step we calculate the average distances for each data subset (well type-fault trend) to produce Table 2, whose results are discussed in a further section.

Parameter	Magnitude	Comments
Average minimum distance between wells and thermal springs	415 m	Maximum distance of 1505 m occurs between well 58D and Erendira hot spring, and a minimum of 24 m in well 2
Average minimum distance between productive wells and hot springs	282 m	Only wells actually integrated to the supply systems to power plants were considered (May 2004)
Average minimum distance between non-productive wells and thermal springs	521 m	A 65 m minimum distance was found for well 42
Average minimum distance between wells and faults (of any trend)	248 m, 197 m omitting wells 20, E1 and E2	Most values are under 500 m, frequent value are around 350 m, values higher than 1000 m occur only in wells 20, E1 and E2. If we omit these wells a relative maximum of 493 m occurs between well 40 and Maritaro fault and a minimum at well 16D, located over the Los Azufres fault trace
Average minimum distance between productive wells and faults	179 m	Maximum of 403 m for well 18. Most wells have a minimum distance associated with E-W faults, excepting wells 5 and 51 (N-S) and wells 17, 28, 37, 42, 46 and 66D (NE-SW)
Average distance from non-productive wells and faults	233 m omitting wells 20, E1 and E2	16 wells associated with E-W faults: 3, 11, 12, 14, 15, 21, 24, 29D, 30, 31, 39, 40, 44, 49, 54, 55 11 wells associated with NE-SW faults: 7, 8, 10, 10A, 10B, 10C, 20, 27D, 27, 47, 50, 58D 1 well associated with N-S faults: well 53
Average topographic height of productive wells	2911 m	
Average topographic height of non-productive wells	2747 m	2773 m if boreholes 20, E1 and E2 are omitted
Average longitude of nearest fault to productive wells	3409 m	
Average longitude of nearest fault to non-productive wells	3318 m	The last two results are consistent with the idea that a longer fault should be more important as a geothermal indicator. In fact E-W trend is composed of individual faults with a greater average longitude, probably because they are younger and their continuity at the surface is clearer. So this behavior could not be a direct consequence of a bigger penetrability associated with a bigger horizontal longitude.

Table 2. Average distance from productive wells to faults and hot springs at Los Azufres, Mexico.

This is a very simple classification scheme, since another attributes of each data set, that can be managed by the system, were not considered, for example for thermal features: temperature, type of manifestation, area or the total heat discharge, and for faults, attributes like: total length, age, vertical offset, etc. Some of these attributes, especially those of thermal features, are not available, but the main reason to omit them in the analysis is that those characteristics have not been used systematically to select drilling sites at Los Azufres, and there are not standard criteria to include them. At this stage of the project, our priority is to systematize the drill location problem using the conventional criteria established at the CFE for this task.

3.2 Contribution of GIS to the identification of hidden faults

The identification of many structures that are difficult to observe by field mapping is other contribution of the data management using a GIS. We conducted the photo interpretation of lineaments that could be associated with hidden faults using Thematic Mapper images, ortho-photographs, digital elevation models (DEM) and geophysical data.

Linear features were photo-interpreted directly on screen displays of satellite images and low altitude ortho-photos, and then included as new geothermal data layers. A photo-interpretation procedure was also used to identify linear features on digital elevation models with resolution cells of 80 m, 30 m and 10 m. Each model was displayed sequentially in the screen as a shaded relief map with different sun angles. The linear features observed more persistently were visually traced. This procedure produced the most useful results for the interpretation of linear features at the surface. Finally we merged the maps of interpreted linear features to produce Fig. 5.

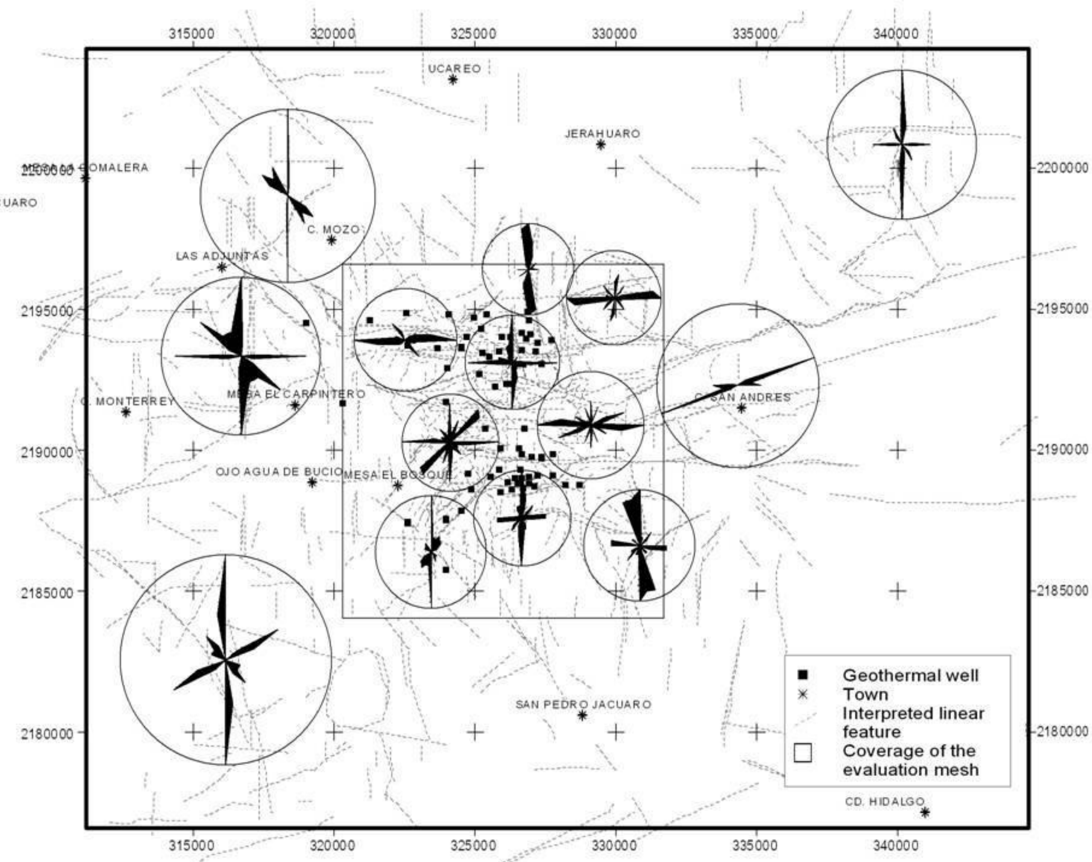

Fig. 5. Regional map showing a composite of linear features interpreted on Thematic Mapper images, ortho-photographs and digital elevation models. Rose diagrams built for the cumulative length of photo-interpreted lineaments show the importance of N-S trend. The coverage of the grid mesh used for Multi-Criteria Evaluation is also shown. UTM coordinates are in meters.

As at Los Azufres a clear cut association between circulation losses at depth and fault traces has not been identified, we have no other way to obtain a plane view of hidden (without superficial expression) geologic structures other than by geophysics. Linear interfaces were identified calculating the horizontal gradient of geophysical maps. In order to make a conservative interpretation we defined linear interfaces as the axes of elongated contours in the horizontal gradient maps.

The implicit assumption underlying this procedure is that high lateral geophysical changes associated with parameters like density, magnetic susceptibility or resistivity, provide a significant insight on the presence of lithologic changes in the ground and when those changes have a linear pattern, the interface can be an evidence of a hidden fault that puts in contact two materials of different properties. Conventionally, we decided to use tics to identify the low resistivity, low density or low susceptibility side of a lineament.

This procedure was applied to the Occam resistivity maps at different depths, in which case resistivity variations can be related to permeability changes associated with variations of alteration percentage, texture or lithologic type in the subsurface (Fig. 6). Differences in height at contiguous soundings are not big enough to difficult this task, due to the non-horizontality of a constant depth map. Gravity and magnetic provided an insight to lineaments of a more regional character with no identified association with the production of fluids.

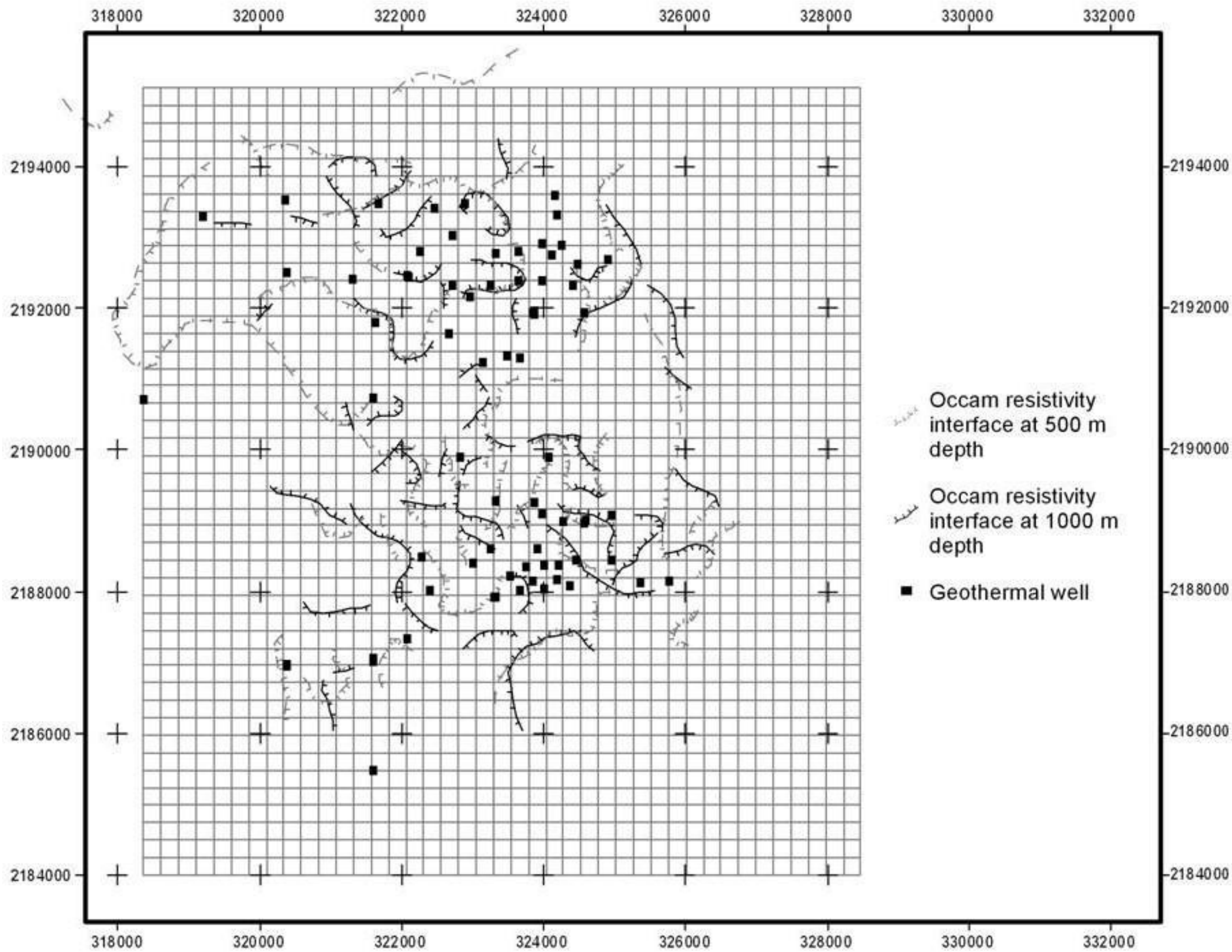

Fig. 6. Interfaces at 500 and 1000 m depth identified as the axes of elongated maximum contours of the horizontal gradient of Occam resistivity. Different weights were assigned to lineaments at each depth. UTM coordinates are in meters.

3.3 Development of a MCE strategy

The application of a MCE method in a geothermal field under exploitation requires the development of criteria to handle a greater variety of data than in the case of regional exploration. On the other hand, each study is constituted by more and better detailed data, and the geothermal significance of each additional property must be interpreted in light of previous drilling results.

For example, data available in a geothermal field under exploitation include parameters measured in wells that depend on the depth (temperatures, pressure, circulation losses, etc.). Detailed geophysical studies like DC, MT or TDEM show also the distribution of resistivity at different levels below the topographic surface. For most geothermal prospecting methods the significance of the data attributes (ranges, depths or orientations, etc.) can vary with time depending on the new drilling results continuously produced. Those attributes cannot be omitted by a realistic study at a field in exploitation.

For the development of a computer assisted methodology to select drill sites it was necessary to study which combination of exploratory parameters could be associated with the different production zones of the field. In the past, we have observed that E-W faults and thermal manifestations, and to a lesser degree, low but not minimum electric resistivity, are the most reliable clues. However, the frequent identification of successful production wells without a clear-cut association with those conditions, or of failed wells when evidence seemed to be encouraging, make it necessary to look for more accurate criteria on the basis of the comparison of a comprehensive exploratory and production data sets.

We departed from the assumption that comparison of maps of each geothermal parameter with production data is the best way we have to define the geothermal significance that each parameter can have to select new drill sites. In this way, we selected a data subset of what we consider the most relevant studies, defined the relative importance of each one, and determined the numeric weights used for the calculation of a geothermal suitability index. As a final step, we extend these results using the same weights defined from the drilled areas to identify the areas with similar geothermal parameters.

To apply the procedure delineated in the previous paragraph, it was necessary to solve practical problems as how to define a representative property of a successful well and how to transform geothermal data into a numeric value suitable for a weighted averaging procedure. Before giving a detailed description of the procedure we followed, we describe the conceptualization on which we based the subsequent development.

We decided to make the evaluation of a 115 km^2 area (10.25 km x 11.25 km) using a regular square mesh of 250 m per side (Fig. 6), and to use vector rather than raster representations of geothermal data. The last criterion was intended to avoid excessive computational requirements and geometric non-compatibility problems due to differences in coverage and data resolution of different variables or of a single parameter at different depths. On the other hand, pixel size analysis is not advisable because, in most cases, local values do not correspond to measured but to interpolated numbers on the basis of unevenly distributed data.

Intensive and extensive attributes

Most features have an extensive property associated with their geometry and one or several intensive attributes (following a nomenclature inspired by thermodynamics). We call ‘extensive’ properties those associated with geometric dimension whose evaluation for each cell can be represented by a cumulative summation of the property of each feature intersecting the cell (for example the total number of points, cumulative length of linear features or the cumulative area of a particular lithologic type). GIS software let us calculate the intersection of the polygons constituting the evaluation grid in which we divide the studied area, and point, linear and polygonal features (geometric shapes utilized to represent geothermal information) in a very fast and accurate way.

We name 'intensive' attributes, those properties of a feature that modify the initial geothermal significance assigned on the basis solely on its extensive property. For example, depth of the resistivity map, temperature or flow rate of a hot spring, or the orientation of a linear feature. Qualitative attributes can be distinguished because the resultant value for several features contained in a cell is better represented by an average than by a summation.

To solve the problem represented by intensive attributes we decided to apply a weighting procedure twice. In a first step, we quantified the extensive attribute of each feature intersecting an evaluation cell and then we made a weighted summation of all contributions. The final result was normalized from 0 to 10. Relative weights were assigned according the interpreter's experience, depending on the intensive attribute of each feature. This procedure was repeated for each data layer. For example, in the case of the photo-interpreted linear features, in the first step the total length of lineaments intersecting each cell was calculated as the summation of each individual intersection and in the second this result was weighted by a factor depending on its orientation.

After normalizing results for each data layer, the second step was to make a weighted linear combination of partial results from each layer and to apply a new normalization to produce values between 0 and 1. The process can be better understood with the following mathematical explanation.

Mathematical procedure used for the MCE method

The (normalized) geothermal index was calculated as:

$$GI_{ij} = \frac{g_{ij}}{g_{\max}} * Nrg \qquad (1)$$

GI_{ij} = Normalized geothermal index for cell *ij*.
g_{ij} = Raw geothermal index in cell *ij*.
g_{max} = Maximum raw score in the evaluation mesh.
Nrg = Normalization range (1 for this study).

where

$$g_{ij} = \sum_k W_k P_{ijk} \qquad (2)$$

g_{ij} = Raw geothermal index for cell *ij* in the evaluation mesh.
W_k = Weight of the geothermal data layer *k*. Assigned on the basis of subjective judgment of personnel involved in the selection of drill sites in the past.
P_{ijk} = Normalized partial geothermal index for cell *ij* due to contribution of layer *k*.

$$P_{ijk} = \frac{p_{ij}}{p_{\max}} * Nr \qquad (3)$$

p_{ij} = Raw score of the partial geothermal index in cell *ij*.
p_{max} = Maximum raw score in the evaluation mesh.
Nr = Normalization range (10 for this study).

$$p_{ij} = \sum_{l} w_l a_{ijl} \qquad (4)$$

w_l = Weight for the extensive property l according to its significance as a geothermal indicator. The significance is based on intuitive knowledge of the field and visual comparison of maps and contours of thermal discharge in wells.

a_{ijl} = Intersection between cell ij and a geometric feature l with a geothermal attribute. It is measured in terms of area for polygons, length for linear features and number of points for point features.

$$a_{ijl} = A_l \cap c_{ij} \qquad (5)$$

A_l = Each of the polygons of constant average value in which a contours map is divided according the data range and its significance as a geothermal indicator (intervals of electric resistivity, hydrothermal alteration percentage, temperature, gradient, etc.), or the subset of lines grouped according a common attribute with geothermal significance (in this study: depth for resistivity interfaces or orientation for photo interpreted lineaments; another potential attributes are the age or composition of the lithologic unit affected by the lineament), or the subset of points with a common attribute (temperature, chemical composition, flow rate, etc.).

c_{ij} = A cell in the evaluation mesh (250 x 250 m square cell for this study).

4. Detailed procedure for the MCE method

The application of the MCE at Los Azufres can be summarized in the following steps. Each one is explained in detail in this section:

1. Selection of a parameter to quantify the success of a drill site on the basis of production data.
2. Identification of the most relevant geothermal data layers to select the drill sites, on the basis of past drilling results.
3. Selection of relative weights for each data-layer selected in step 2 to combine their individual values into a resultant single number in step 6.
4. Selection of relative weights to transform the combined intensive and extensive attributes of each feature in a layer to a number in step 5 (for example to take account of the orientation of linear features, or the resistivity of an area at a fixed depth).
5. Calculation in each cell in which we divided the studied area, of the (partial) contribution of a layer to the suitability index considering the coverage of each feature (extensive attribute) and their properties (intensive attributes). Summation of the contribution of all the features or parts of them intersecting each cell and normalization of results.
6. Calculation of a geothermal index. Weighted linear combination of the numeric value corresponding to each data layer (resulting from step 5) using weights selected in step 3, and normalization of the final result.
7. Criteria for specific drill site selection from practical considerations (selection of the best drill cells with the same range of geothermal index according the interpreter experience and additional considerations, for example distance to production wells, location of respective fault planes at depth, etc.).

4.1. Selection of a parameter to represent the success of a drill site

For this task, it was necessary to decide which parameter could be considered as the most representative of a successful drill location. Maximum temperature, enthalpy and steam production for each well were under consideration but finally we decided to use total thermal discharge (the product of mixture enthalpy and total mass discharge at separation pressure) as the most representative parameter (ninth column in Table 1) (Fig. 4), because this parameter combines not only the specific energy supply but also the amount of mass extracted. Corrections to take into account differences in separation pressure were not applied because we are interested just in a bulk behavior on the operative conditions on which they were evaluated.

We divided the variation range of this property into three intervals. Values below 50 MW were considered as an indicator of a moderately successful drill site, values from 50 to 100 MW were considered as good drill sites, and values from 100 to 200 MW were considered as excellent drill sites. The limits of each interval are subjective; we selected them considering the relative conditions prevailing at Los Azufres and consequently they may be inappropriate for other fields.

From the viewpoint of geothermal exploration, even thermal discharge at wells that are not used for electricity generation is of interest to evaluate the significance of each geothermal exploration method. Unfortunately, these data were not available for the present study, so our definition of a “successful drilling site” is biased by criteria dependant of present day production policies. Although the thermal discharge of wells rejected by production policies were not used to define the success of a drilling site, other parameters measured in those wells were used to locate new drill sites, as explained in the following paragraphs.

4.2. Identification of the most relevant geothermal data sources (layers)

Even though we have the computational capability to include an exhaustive data set to make this evaluation, we consider that it would not be a worthwhile procedure as long as we do not have a clear idea of the geothermal significance of each data source. That depends on studies that we have just started. For the moment, we had to rely on subjective criteria based on experience and trying to profit of the efficient display capabilities of the GIS to compare maps of different parameters.

In the case of numeric variables like resistivity, temperature or hydrothermal alteration, we made a visual comparison of contour maps at different depths with those of the thermal discharge measured in wells (Fig. 4), with the aim to select variables whose contours show what we visually considered the most similar patterns. Criteria to apply numeric methods for map correlation are under study as part of a statistical research in progress.

On the basis of these comparisons, and our past experience at Los Azufres, we selected the following data layers as the best indicators to locate successful drill sites (third column in Table 3): interpolated contour maps of thermal discharge, maximum stabilized temperature, stabilized temperature at 500 and 1000 m depth, maximum average thermal gradient, Occam resistivity at 1000 m depth, total percentage of hydrothermal alteration at 1000 m depth, fault planes between 700 and 2000 m depth, distance to thermal manifestations, superficial hydrothermal alteration, resistivity interfaces and photo-interpreted lineaments.

Meters above the sea level (masl) is the basic coordinate reference system for the development of conceptual models of geothermal fields, reservoir simulation or 3D displays of subsurface geometry. Consequently it is the reference system used in the GIS database. However, for the development of the MCE method we decided to use maps at constant depth in meters below the ground surface, because our final objective is to locate drilling sites, and depth is one the most important economic criteria to decide the location of a geothermal well. In other words, our objective is the comparison of the geothermal suitability of different sites at the same depth.

Working with maps at constant depth we avoid the problem of designing a terrain correction for the geothermal index resultant of the evaluation of maps at constant height, and preserve the customary work style for drill location at the CFE. Another reason is that in the area covered by our study (Fig. 2), heights vary from 2300 to 3200 masl (a maximum difference of 900 m) and for the shallow production intervals (400-700 m depth in well 41), relevant maps at constant height are over the topographic height of areas surrounding the production zone. Production in most wells occurs at depths where maps at constant height are difficult to handle as they represent conditions at depths with a difference of several hundred meters.

Layer	Intuitive Relevance	Parameter Description	Weight	Feature type	Extensive attribute	Intensive attribute	Relative weight
1*	1	Thermal discharge from extracted fluids [MW]	8	Polygon	Area	20-50 MW 50-100 MW 100-200 MW	1 3 6
2*	2	Maximum stabilized temperature [°C]	7	Polygon	Area	100-200°C 200-260°C 260-360°C	1 3 6
3*	2	Stabilized temperature at 1000 m depth [°C]	7	Polygon	Area	75-120°C 120-180°C 180-240°C	1 3 6
4*	3	Temperature gradient (maximum temperature/depth to maximum temperature) [°C/m]	6	Polygon	Area	0.02-0.15 °C/m 0.15-0.20 °C/m 0.2-0.65 °C/m	1 3 6
5*	3	Stabilized temperature at 500 m depth [°C]	6	Polygon	Area	30-60°C 60-120°C 120-170°C	1 3 6
6**	3	Faults [m^2/evaluation cell]	6	Polygon	Area	NE-SW, NW-SE N-S E-W	1 3 6
7**	4	Occam resistivity at 1000 m depth [log_{10}(Ohm-m)]	5	Polygon	Area	1.4-1.8 log_{10}(Ohm-m) 0.6-1.2 log_{10}(Ohm-m) 1.2-1.4 log_{10}(Ohm-m)	1 3 6
8**	4	Location and temperature of surface thermal features	5	Polygon	Area	25-40°C 40-70°C >70°C	1 3 6
9**	5	Occam resistivity at 500 m depth	4	Polygon	Area	1.6-2.1 log_{10}(Ohm-m) 0.6-1.0 log_{10}(Ohm-m) 1.0-1.6 log_{10}(Ohm-m)	1 3 6
10*	5	Total hydrothermal alteration percent at 1000 m depth [%]	4	Polygon	Area	0-60% 90-100% 60-90%	2 3 5
11**	5	Lineaments of high horizontal gradient of Occam resistivities	4	Line	Length	2000-2500 m depth 500-1500 m depth 1000 m depth	2 3 5
12**	6	Superficial hydrothermal alteration	3	Polygon	Area	non-differentiated	1
13**	7	Cumulative length of photo-interpreted linear features at surface	1	Line	Length	NW-SE, NE-SW N-S E-W	1 3 6

* Data from drilled wells **Data from pre-feasibility studies

Table 3. Numeric classification of parameters with attributes of geothermal significance, and their relative weight for the calculation of a geothermal index to measure their suitability as a geothermal indicator.

4.3. Selection of relative weights for each data source (layer)

As explained before, two sets of numeric weights were selected. The first one related to the relative geothermal significance of each layer (fourth column in Table 3), and a second one, associated with the relative significance of features within a single layer depending on their intensive attributes (last column in Table 3). Even though at its present stage assigning of weights for the MCE procedure relies on interpreter intuition and experience, efficient display capabilities of GIS made possible the visual comparison of a much more comprehensive set of data than ever before.

In the fourth column of Table 3 we present the relative importance of each selected variable using a numeric scale from 1 to 10. It is important to notice that we decided not to restrict the summation of those numbers to a given value because we considered that variables are not mutually exclusive, it is to say that the presence of one of them does not preclude the presence of the other. Several variables, for example faults and thermal features, are interrelated and could provide redundant information but we cannot avoid this possibility until the statistical study in progress is concluded. On the contrary, weights in the last column were restricted to produce a 10 units sum because they are mutually exclusive as far as a single feature cannot have two different values of the same property at the same time.

4.4. Selection of relative weights for the properties (intensive attributes) of each data layer

Maybe the most difficult task faced in implementing the MCE was the way to transform contoured data to a numeric value representing their geothermal significance, on the basis of their absolute value, depth, and area extent.

Parameters that can be represented by contour lines were treated as polygons whose boundaries were constituted by contour lines of user-specified values. Usually we divide the contours range (the counter domain in mathematical language) in six intervals. We use the contours with the extreme values in the corresponding interval as the boundary of the polygon, and assign the average of limiting contours as their numeric attribute.

The area of intersection between each polygon with an evaluation cell was multiplied by the weight assigned to the intensive attribute (last column in Table 3) before doing the summation of the contribution of all the polygons intersecting each cell. That procedure was applied, for example, in maps of Occam resistivity, stabilized temperature, percentage of total hydrothermal alteration, maximum average gradient, and total thermal discharge. Even though we know that the interpolated values of data measured in geothermal wells may not be realistic, we decided that it is the best way we have at this moment to take well data into consideration to locate new drill sites.

Each data layer is evaluated separately and results for each cell in the evaluation mesh are stored as entries of an array's column. In that way, an adequate selection of columns makes possible the evaluation of the geothermal suitability at specific depths or with a subset of layers of specific interest for a user. We are not interested in a particular depth but in a depth interval, and for that reason we combined results of the data layers in the final suitability index.

For studies whose attribute is a numeric property, i.e., those measured with an interval or ratio scale (Davis, 1986) (for example, temperature of a polygon bounded by isothermal contours), normalized values of the numeric attributes can be used directly as the weighting factor for the extensive property, a procedure easy to apply when there is a monotonic relation between the property and the geothermal significance, as is the case of hot spring temperatures. However, in some cases, the attribute is not a numeric type, i.e., it is measured with a nominal or ordinal scale (lithology or lineament orientations, for example), the relationship is not so clear (total hydrothermal alteration percentage) or the relationship is not monotonic (as is the case of resistivity at Los Azufres where low but not minimum values are the best geothermal indicator).

For this study we preferred to make discrete the interval of variation of the intensive attribute in several contiguous intervals assigning a constant weight for each one (for example the orientation of linear features grouped by cardinal points, or temperatures grouped into three contiguous ranks). This procedure was suitable also for qualitative (non-numeric) attributes or for numeric properties that do not have a monotonic significance as a geothermal indicator.

By visual inspection we identified the attribute interval corresponding to each production level. Contours of the variable (or qualitative attribute of the features) corresponding to low thermal discharge wells were qualified with the lowest numeric values, those corresponding to the medium thermal discharge level were given a medium weight and attributes corresponding to wells with the highest thermal discharge, were assigned the highest weights (sub-cells in the last column of Table 3).

4.5. Evaluation of the partial contribution of each data layer

Point features

The only point features included in the evaluation were thermal manifestations (Fig. 3), whose only considered attribute was temperature (acid character of hot springs makes difficult to find a direct relationship with solute geochemistry without a detailed data interpretation). However, as we considered that most of them are surrounded by steaming grounds, we preferred to treat them as polygonal features that have an influence area represented by a 250 m perimeter. An accurate map of surface thermal features should be very useful to improve this task at Los Azufres.

Linear features

Linear features included photo-interpreted lineaments (Fig. 5) and linear electric resistivity interfaces at different depths (Fig. 6). In the first case, orientation was considered an important attribute and depth in the second (see Table 3). Taking into account that the accuracy of resistivity data decreases as depth increases and the fact that resistivity interfaces at 1000 m depth are the most representative features of production depth at Los Azufres, we assign the additional weights depending on depth as indicated in Table 3.

Linear interfaces identified on potential field maps (gravity and magnetic) were not evaluated thus far, as we have not determined whether they have a direct association with the well production. However, we considered them to define the specific drill sites after calculating the geothermal index.

Polygonal features

Polygonal features constitute the biggest group, as these features comprise thermal spring areas, fault planes, and polygons formed from contour maps.

Field-mapped faults were treated not as linear features (attending only their superficial trace) but as surfaces. We started calculating the three-dimensional geometry of fault planes at production depths (700 to 2000 m), then we projected these planes on the horizontal and measured the area of intersection of the projected area with each cell in the evaluation mesh. We consider that this is a more representative geothermal indicators that the length of the trace at the surface or a symmetric buffer around its trace at the surface. We used the conventional inclination (82°) to calculate the faults geometry in the subsurface; this value could be modified on a fault by fault basis if these data were available in the future. Additional weighting was used on the MCE method on the basis of fault orientation (Table 3, columns 7 and 8).

As it can be seen in Table 3, stabilized temperature contours were recognized as the second data source in importance, only after the interpolated values of thermal discharge. For that reason contours at several depths were considered and they received a relatively high weight. The reason for that decision is that we are using equilibrium temperatures and we consider this property is a reservoir parameter more suitable to be interpolated, as they represent equilibrium conditions with a smaller spatial variability than production data (fluid flow rates or production temperature, for example).

Maps of maximum stabilized temperature and temperatures at 500 and 1000 m depth were used for this evaluation. They were calculated by the interpolation of temperatures estimated using the Horner method, applied to the temperature log series measured during drilling breaks (García-Estrada *et al.*, 2001) in order to compensate the thermal disturbance due to the drilling mud circulation. Due to the characteristics of production wells and the high thermal gradients at Los Azufres, very long times of rest after drilling is completed, produce temperature gradients associated to free convection inside the hole and are not representative of the natural conditions of the surrounding rock. The use of those disturbed temperatures non representative of the original thermal field but of the well under production conditions is considered through the thermal production data.

Production temperatures were not used because the depths at which they are measured do not correspond to the original temperature field, and on the other hand, data corresponding to production conditions were captured using the heat discharge values. Temperatures were treated in the same way as Occam resistivities, so that the area of each cell covered by a polygon of constant temperature was weighted according the discrete rank indicated in Table 3.

Additionally, we used an artificially created variable consisting of the ratio of maximum temperature and depth at which it is found. This is a temperature gradient whose value increases when a high temperature and permeable zone is near the surface, separated by an efficient impervious layer. We consider that interpolated values of this variable are a better indicator of shallow permeability from a global perspective than a parameter based on local conditions as the circulation losses. Obviously areas of maximum interest are those where this ratio is highest. We did not explicitly use circulation loss data because we consider that it makes no sense to interpolate those values for areas where drilling data are not available. Circulation losses are more related to discrete fault planes at depth, which were considered separately.

Occam resistivities for several depths were available, but only those at 500 and 1000 m below surface were considered. Each map was treated as a separate data source (layer) for which each polygon intersecting a grid cell was weighted by the resistivity value interval. Weights take into account our experience at Los Azufres, where observations confirm the model that relates minimum resistivities to clay deposits confining the top of the reservoir (cap rock), while low but not minimum resistivity values correspond to the reservoir at depth. Representative resistivities of those conditions vary with depth, as can be observed in Table 3 (columns 7 and 8).

Total hydrothermal alteration percentage at 1000 m depth was also considered. Weights reflect the fact that high values are frequent in production depths, but highest values imply that permeable zones can be sealed. A more detailed treatment is recommended using recently available databases including the abundance of different alteration minerals. A study conducted to compare Occam model resistivities calculated for time domain electromagnetic and Schlumberger soundings with hydrothermal mineralogy in wells at Los Azufres, shows that the clay content is a parameter very nearly related with the modeled resistivity (García-Estrada, 2005).

4.6 Calculation of the geothermal index

Calculation of the geothermal index was conducted in a six-step process. In the first step, points, length or area of each feature that intersects an evaluation cell was determined, and in the second, the extensive measure for each feature was multiplied by the factor indicating its geothermal significance (last column in Table 3). In the third step, the resulting values for all features from a single layer in each cell were summarized, and in the fourth step, resulting values were normalized (between 1 and 10) using their extreme values in the studied area. This process was repeated for each geothermal variable indicated in the third column of Table 3. After concluding the evaluation for all variables, the fifth step was to calculate a weighted average (weighted linear combination) of the contribution of all the layers using the weights indicated in the fourth column of Table 3, and finally the sixth step was the normalization (between 0 and 1) of the resulting value to produce the geothermal index.

Results of the fourth step were used to compare the contour maps resulting from the summation of pre-feasibility and post-drilling data layers (Fig. 7). In Figure 8 we present the ‘raw geothermal suitability index’ calculated as the normalized sum of the joint pre-feasibility and post-drilling data layer sets (sum of Fig. 7a and 7b normalized between 0 an 1), and the weighted geothermal index is presented in Fig. 9.

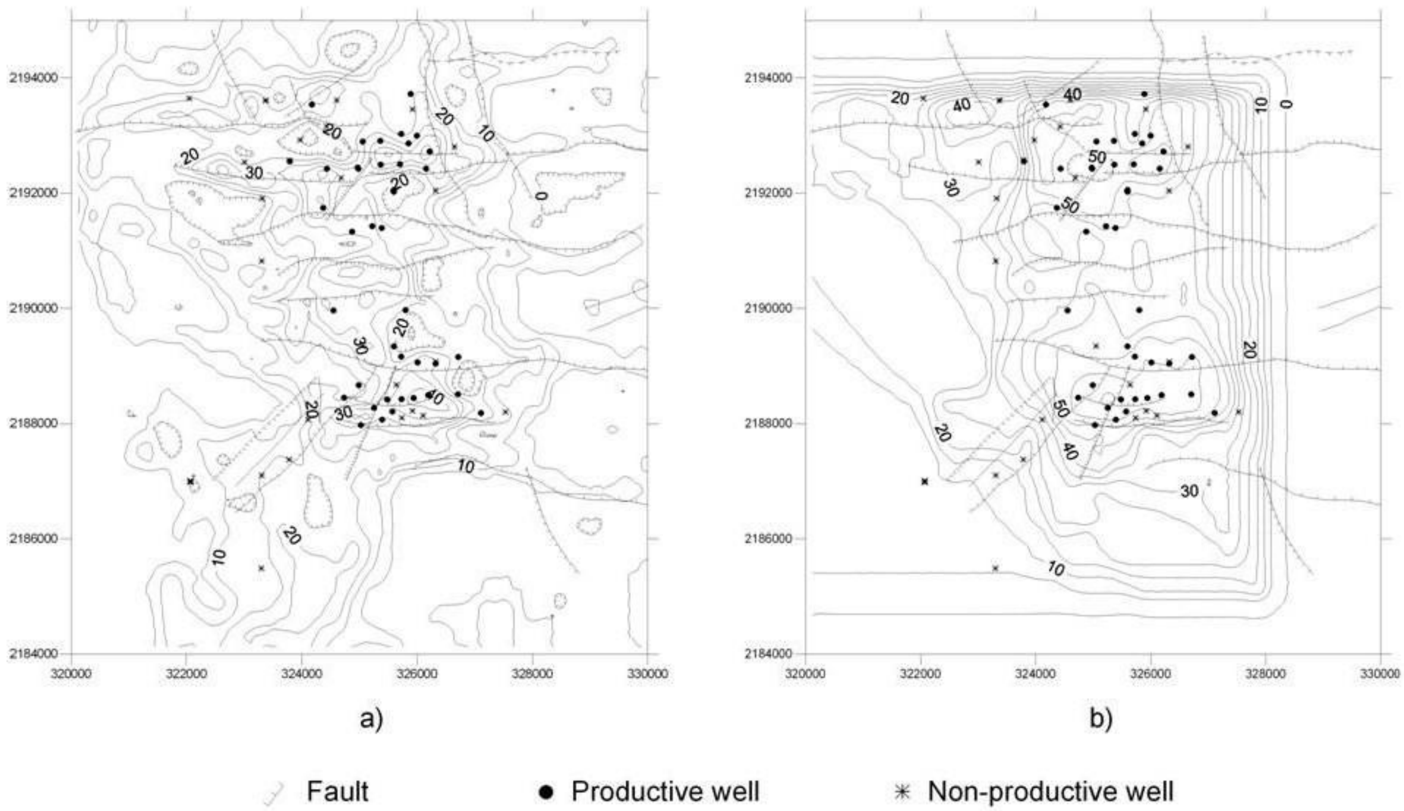

Fig. 7. Comparison of the raw geothermal feasibility index, non-normalized, resulting from pre-feasibility (a) and well drilling (b) geothermal data listed in Table 3. Values calculated as the sum of the standardized values (from 0 to 10) for each layer. Production and non-production geothermal wells are shown. See text for a complete discussion. UTM coordinates are in meters.

Cells in the evaluation mesh outside the coverage of a particular layer received a null contribution from that variable, so, cells far away from the production area could be undervalued, as they are covered by a smaller number of studies. That originates a bias of the geothermal index toward cells located in the central area of the field. However, most pre-feasibility studies cover an area much larger than the exploited zone, and that let us make at least a relative comparison of the index in areas with similar data information layers.

4.7 Software and hardware

Calculation was accomplished by means of a combination of user programs developed by the authors of this project, freeware and commercial GIS software. We have stressed the development of subroutines that can be translated to the specific software available at different CFE areas. When this study was made, the best developed version of the system was installed in a desk top 3.0 GHz CPU Pentium 4 equipment with 1.0 GB of RAM. Software included the ArcView© 3.2 GIS with the Spatial Analyst extension and user programs in Avenue programming language (a migration to ArcMap© is under study).

Freeware subroutines for MCE, available in the ESRI home page (http://arcscripts.esri.com/) were useful to efficiently conduct the first, fifth and sixth steps of the procedure. The “most geothermal” step consisting in transforming the geothermal evidence to a numeric format using the intensive attributes (step 2), was conducted by means of user software in the Avenue programming language. The most difficult task from the programming point of view, consisting in the quantification of the area of intersection of geothermal polygons with each cell in the evaluation mesh, was conducted with the commercial extension for spatial analysis for ArcView© software[1].

5. Results

5.1 Effect of distance from producer boreholes to thermal features and faults

The results of a distance analysis between thermal springs, faults and wells (Fig. 3) are reported in Table 2. Results show a 0.51 success ratio for wells conceived to intercept E-W faults (17 production, 16 non-production), compared with a 0.35 ratio for wells conceived to intercept NE-SW faults (6 production, 11 non-production). However, two wells associated with N-S faults were successful and just one failed, giving a ratio of 0.66. This shows that the preference to locate new production wells to intercept E-W fault system respective to NE-SW trend is justified. However, the situation is not clear with respect to the N-S trend, because this system is difficult to map in the field, few features have been identified by field work, and then we have a very small sample of wells associated with that trend.

A study of the influence of fault intersections over production data was attempted; however, the number of wells associated with fault intersections (point in the intersection of fault traces) is not enough to obtain concluding results. On the other side, a thorough study requires the analysis of the 3D-line defined by the intersection of fault planes at depth that is beyond the objectives of our study at this stage.

Results in Table 2 show that production wells have an average minimum distance from thermal manifestations and faults that is smaller than for the non-productive wells, even for the most recently drilled wells. That means that regardless our improved knowledge of the field, new geophysical studies and borehole data, there is still a considerable dependence between productive wells and the distance to those superficial features. This situation is partially due to the criteria applied to locate drill sites during the initial exploitation of the field, based essentially on the presence of hot springs, but also to the fact that even when actually the distance to hot springs is not quantitatively considered to select a drill site, if we look for the intersection of E-W fault traces and electric resistivity lows, the selected sites have a tendency to be located near the hot springs. This is not an obvious result, if we consider that the wells were located to find production conditions (enthalpy, temperature and flow rate) at depth, and even so, a correlation with thermal features at surface persists. On the other side, these results suggest that there is some kind of redundancy in the information provided by the different data layers.

5.2 Interpretation of linear features

Figure 5 shows the superposition of all the interpreted linear surface features. Some of them correspond to the same feature but identified independently in different images, a situation that explains the small differences in the trace.

We consider that the redundant identification of some lineaments using very different technological media diminishes the subjectivity of interpretation, so we decided to preserve repeated features in the analysis as a

---

[1] The reference to commercial software is intended only for descriptive purposes and does not imply any endorsement by the authors. Several GIS packages can be well suited to execute the task but the amount of user programming could vary.

way to give additional weight to more reliable features. It was surprising the amount of features not previously mapped.

Rose diagrams of the photo-interpreted lineaments show that the cumulative length of the E-W trend is dominant only in the topographic high occupied by the geothermal field, but in general lineaments show a dominant N-S trend (Fig. 5). Higher cumulative length of N-S features in the geothermal field area results from their abundance, in spite that most N-S linear features have a smaller individual extent than those trending E-W. The apparent lack of continuity of N-S trending features respective to E-W can result from the age of faulting that seems to be older in the former case, as can be deduced by the age of rocks affected by this trend outside the geothermal field. However, in the studied area fault reactivation makes it difficult to apply this criterion.

At Los Azufres the most intense thermal features are located in the outcropping Pliocene andesitic unit (Andesita Mil Cumbres) and not in the less permeable Quaternary rhyolitic rocks. Consequently, we consider that the age of rocks affected by faulting is not an adequate criterion to evaluate the geothermal significance of faults in this geothermal field. Anyway, the programs we have developed are prepared to assign different weights for faults depending of the age or lithologic type of the intercepted rocks, a criterion that we consider useful to locate the best geothermal prospect on feasibility studies at a regional scale when no additional age information is available.

Resistivity interfaces are shown in Fig. 6. Just a few of them observed at 500 m depth persist in the 1000 m depth. They can correspond to more penetrative faults and for the same reason can have a more ‘regional’ character. Linear features at greater depth have a tendency to be shorter, suggesting that there is a smaller horizontal homogeneity of resistivity at greater depth. As we expect to have a more homogeneous thermal field at depth than near the surface, because we are nearer the heat source (a hypothesis requiring further analysis), homogeneity at shallow depth can result from a greater homogeneity of hydrothermal alteration near the surface. Noise due to lateral effects on Schlumberger soundings is another cause that needs further study.

Conclusions of the distance analysis from producing wells to faults and surface thermal features, and linear features shown in figures 5 and 6, are used as judgment elements and raw data integrated in the MCE analysis whose results are described in the next section.

5.3. MCE Results

High absolute values in Fig. 7a and 7b occur in cells where more individual data layers (of their respective subset) provide consistent favorable geothermal evidence. The number of post-drilling data layers (6) is smaller than that of pre-feasibility studies (7), but their results are more consistent and consequently produce higher geothermal suitability values reaching a maximum around 60 units, meanwhile the pre-feasibility layers reach only 45 units and the zones of high value cover a smaller area. Contours above 20 units delineate areas of geothermal interest in Fig. 7a, while values over 45 units seem to play that role in the post-drilling layer data (Fig. 7b).

Contours corresponding to the after-drilling layers are smoother than those of the pre-feasibility data. Two non excluding explanations for this fact are the availability of a smaller number of sampling data to interpolate post-drilling results and a real increase of homogeneity at depth. The steep gradient of aligned contours observed in Fig. 7b is a border effect associated with the coverage of interpolated drilling-data maps.

No single layer has a dominant effect over the contours, except on a local scale, where favorable geothermal evidence from other layers is scarce or where there are not data from other layers. See for example the influence of the hanging-wall block of faults (using conventional terminology of structural geology, after Marshak and Mitra, 1988) in the east of Fig. 7a. The areas of maximum geothermal interest shown in Fig.7b are similar to those shown in Fig. 7a. This result demonstrates that the identification of the best production areas, Maritaro and Tejamaniles, could be done using solely the pre-drilling data layers translated to numeric format, with no need of the weighting average, and the procedure to transform geothermal evidence to numeric values proposed in this paper is adequate.

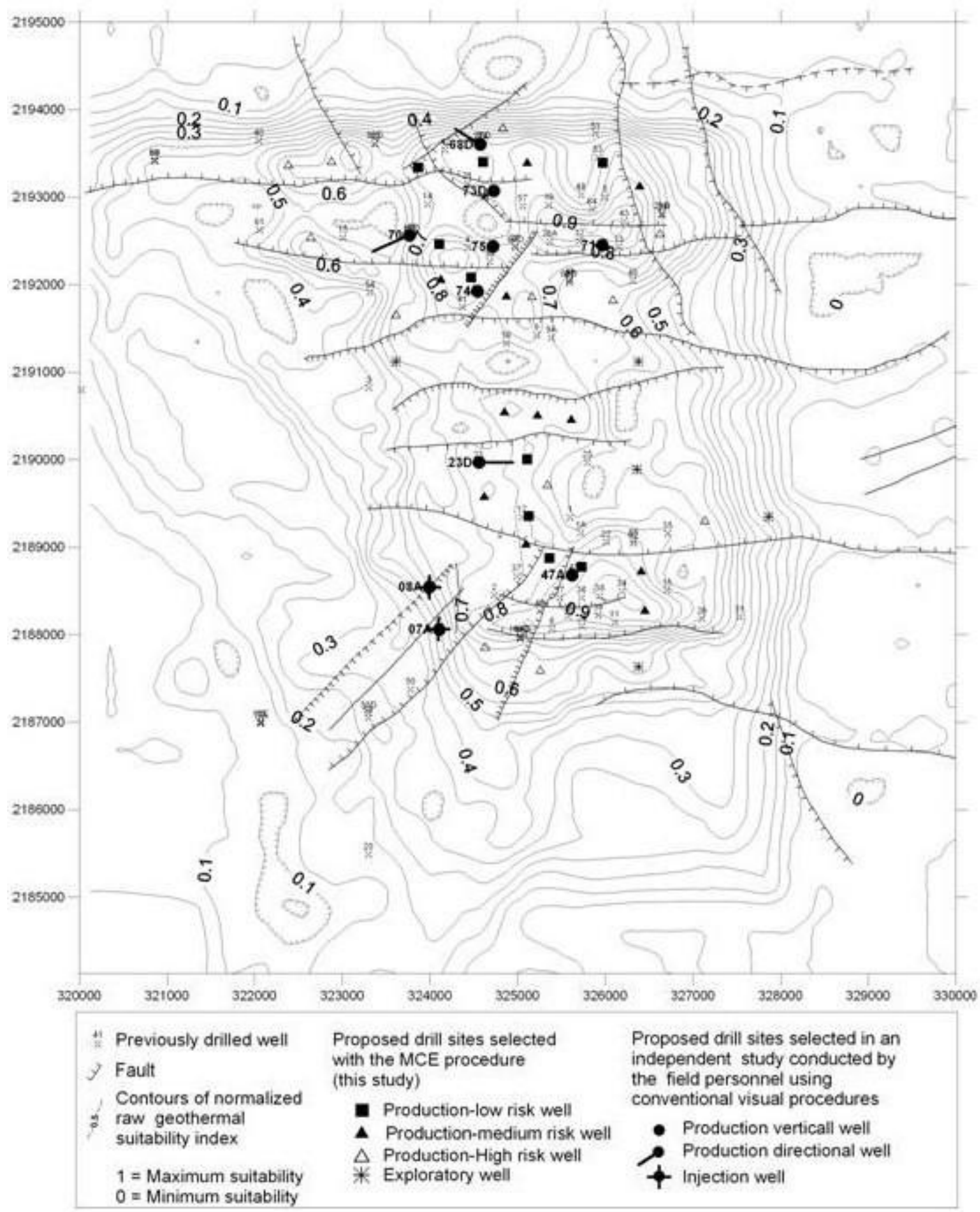

Fig. 8. Non-normalized raw geothermal index obtained as the sum (without additional weighting) of pre-feasibility and drilling-data layers, each one standardized in a scale from 0 to 10 (algebraic sum of maps 7a and 7b). New drill sites proposed by this study are compared with those selected by the field personnel applying conventional methods. UTM coordinates are in meters. See text for a complete discussion.

The decision to include additional criteria to calculate a geothermal suitability index must be considered as an attempt to discriminate the best relative drill locations inside the areas of maximum interest and outside the best zone, where evidence provided by different layers is not consistent or even contradictory, and consequently the geothermal suitability cannot be represented by a simple summation of favorable evidence. The need to apply a weighting procedure to calculate a geothermal suitability index (step 5) diminishes if the weights used to transform geothermal evidence to numeric format are selected adequately.

The summation of the numeric values corresponding to the complete set of data layers (or equivalently the sum of maps in Fig. 7a and Fig. 7b) normalized to produce values between 0 and 1 conducts to Fig. 8, which is a raw geothermal index in which all the previously normalized layers have the same weight. Local maximum anomalies in the production area are similar in figures 7a and 7b and consequently they appear enhanced in Fig. 8. A contour map of the non-normalized index gives a better picture of the absolute amount of favorable geothermal evidence existing at each site (figure not included) but the map with normalized values between 0 and 1 makes easier the comparison of the relative geothermal importance of different sites.

In Fig. 8 some productive wells show middle rank values of geothermal index, but none of them is located in the lowest rank. Most failed wells are located in cells with medium to low geothermal index, but some of them are located on middle rank cells and just a few (wells 11, 24, 30, 39 and 55) are located in cells with a high geothermal index.

In the case of well 11 it is clear that the discrepancy is explained because it was abandoned due to blow-out problems during drilling, but the borehole was located in an excellent location. In the other four cases it is difficult to explain that inconsistency. What is clear is that we have not included a geothermal data layer that properly discriminates those wells as not productive. However, we consider that drilling difficulties are the most likely explanation for the failure of these wells because none of the data layers included in this study, nor other data available in the GIS, provide discouraging evidence; so, the inclusion of a layer containing drilling conditions data may be necessary to discriminate those sites.

Locations of known productive wells have high values and far from the geothermal field, the geothermal index is low. As we know that wells E1, E2, 10 and 20 are definitely outside the reservoir we postulate that index values under 0.3 represent areas of null interest.

An index between 0.3 and 0.5 is observed where the evaluated data layers gave place to geothermal areas unsuitable for the location of productive wells, and values from 0.5 up to 1 indicate areas of real geothermal interest. We consider that the lowest range (0.5 to 0.62) comprises areas of highest risk and the wells located in them have an exploratory character. Index values between 0.62 and 0.75 indicate moderately risky zones, and index values between 0.75 and 1 are the lowest risk locations. The high index sites should be considered as the best locations for drilling new productive wells in the short term. Fig. 8 shows the location of proposed drilling sites based on the raw geothermal index (normalized) and technical considerations discussed later.

Figure 9 shows a contour map of the normalized (between 0 and 1) geothermal suitability index calculated by means of the weighted average of normalized (between 0 and 10) contributions from all the layers (step 6 described in section 4). The inclusion of weights produces cells with absolute values quite different to those obtained when no weights are used, but this effect is eliminated by the normalization. The visual comparison of figures 8 and 9 shows that the inclusion of weights has a small effect in the relative value of cells and consequently contours in both figures show the same general pattern. This result can be produced because weights selected on the basis of a intuitive criteria (Table 3, column 4) have relative values that makes the contribution of different layers compensate each other or because they have a homogeneous effect over most evaluation cells. The use of the pairwise matrix (Saaty, 1977) or principal eigenvector techniques to study this fact or to select a new set of weights is advisable. Ideas proposed by Coles *et al.* (2004) could also be applied to compare results obtained by different interpreters.

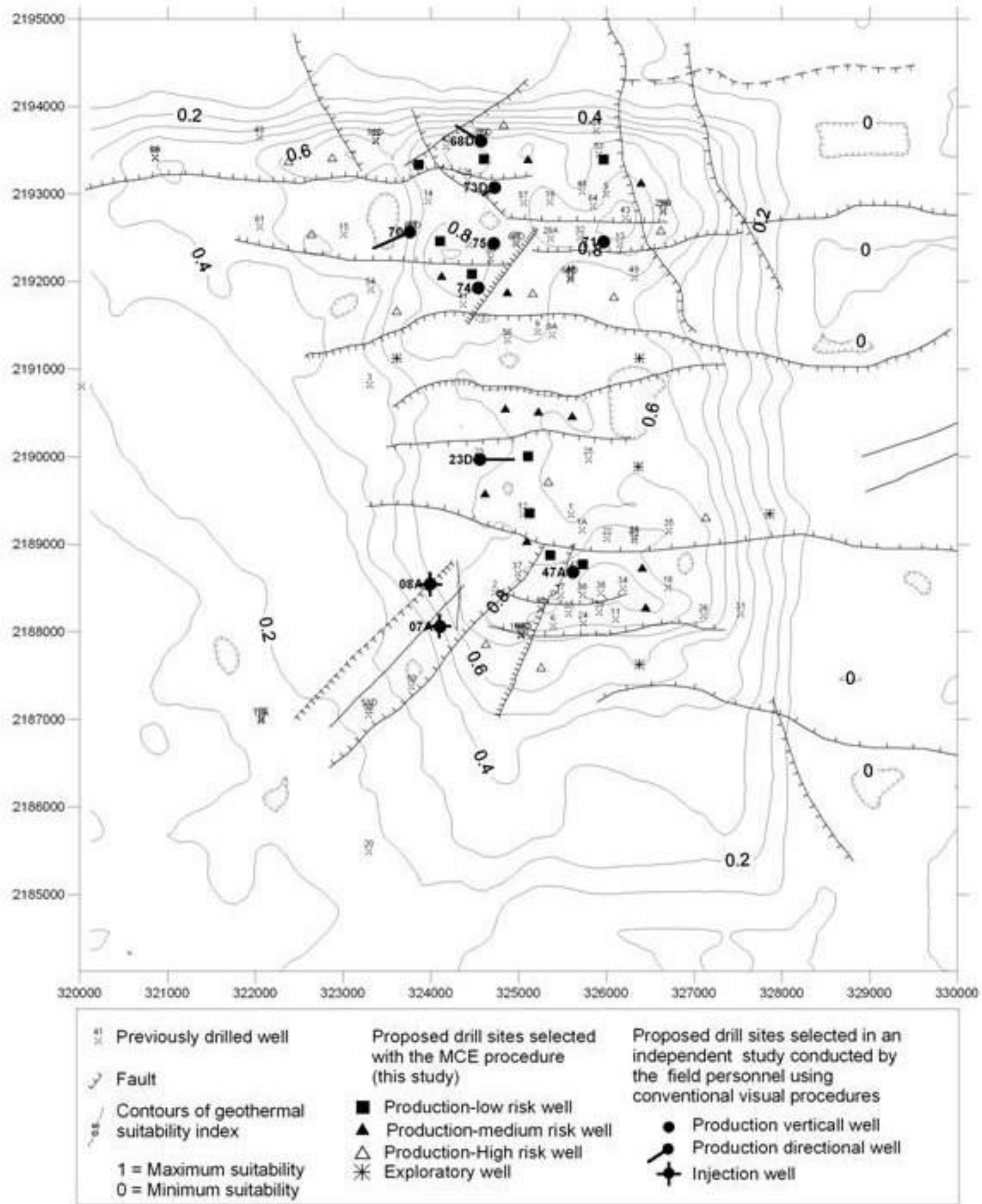

Fig. 9. Normalized geothermal index resulting from the weighted average of the joint contribution of pre-feasibility and post-drilling layers. New drill sites proposed by this study are compared with those selected by the field personnel applying conventional methods. UTM coordinates are in meters. See text for a complete discussion.

The calculation of a residual map as the difference of Fig. 9 and Fig. 8 (Fig. 10), shows values in the interval [0.1,-0.1] that are too small to be significant on a local scale, considering the subjectivity implicit in the MCE procedure. However, it is interesting to notice that there is a consistent trend to obtain higher values in Fig. 9 than in Fig. 8 to the west of the Tejamaniles area, to the north of the Maritaro area and to the west of the known production area, while values diminishes in the east of Tejamaniles and in the central zone of Los Azufres. We think that areas of relative increase of the geothermal suitability index in Fig. 9 respective Fig. 8 occur due to favorable evidence provided by resistivity and stabilized temperature layers, while decrease occurs by the absence of thermal features and the low weight assigned to the photo interpreted lineaments.

As can be seen in Table 3, the interpolated values of thermal discharge have a relatively elevated weight (8 in a 1 to 10 scale). However, taking into account the relative weight assigned to the different data layers, that value should represent only 13% of the maximum value of 63 points (before normalization) that could be achieved in an hypothetical evaluation cell in which all the layers had the best geothermal conditions to locate a drilling site using a weighted average (Fig. 9). The relative contribution of this layer reduces to 8% when weights are omitted in the averaging procedure (Fig. 8).

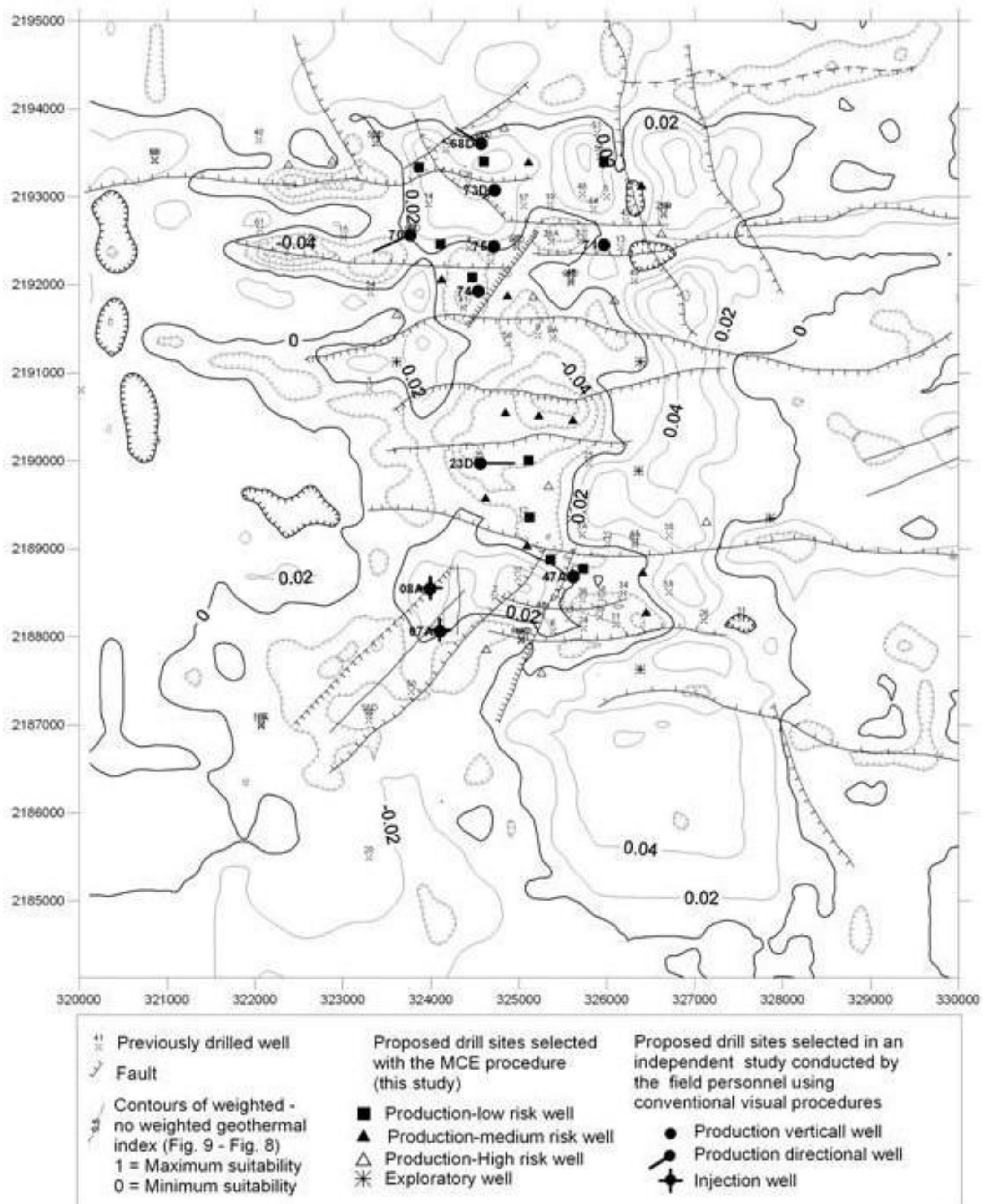

Fig. 10. Map of differences between the geothermal index calculated as a weighted average (Fig. 9) and the raw geothermal index based on a non-weighted average (Fig. 8) of the same layers each normalized between 0 and 10 values.

If we consider the cumulative effect of subsurface data from wells, their relative contribution raises to 37% for a weighted index and 46% for a non-weighted index. In both cases post-drilling data have a smaller contribution than the pre-feasibility data because weights increase the relevance of pre-feasibility data in the final evaluation. In our opinion this criterion is adequate because we are committed with the location of new drilling sites where pre-feasibility studies provide the basic measured data. Post-drilling data play a dual role as a data set to calibrate pre-feasibility studies and as a collateral insight of subsurface conditions through its interpolated values.

This means that regardless the evaluation can be biased to the identification of the well known exploited areas, there is a considerable margin for the contribution of other geothermal data. Bias toward the better studied area is unavoidable because the amount and quality of data is much better were we expect to have the best geothermal conditions. Anyway, relative values of the geothermal index in areas outside the drilled area are useful to estimate the geothermal suitability of each location compared with other sites in the region with the same amount of data.

The conclusion that we obtain from this comparison is that most productive wells are related to high values of the geothermal suitability index even if drill data layers are excluded in the calculation, while most non-producing wells are located in low suitability contours or in the flanks of the local highs.

On the basis of a well-by-well analysis we found that exceptions to this behavior are due to any of the following causes: limitations due to the spatial resolution cell in the evaluation mesh, drilling difficulties that produced failed wells in sites with good geothermal conditions, and, in a few cases, unexplained local conditions that cannot be discerned with the available data.

Differences between Fig. 9 and Fig. 8 are small, and the location of drill sites using any of these maps produce similar results. We preferred the second one to eliminate the additional subjectivity produced by the selection of the additional set of weights involved in the calculation of Fig. 9.

6. Discussion

Conceptual models of the Los Azufres geothermal field and the MCE method to locate drilling sites depart from the same basic geothermal data set, and consequently results must be consistent. That this is so, can be seen from the fact that two main high suitability areas occur to the north and south of the field, related by a narrow corridor of slightly smaller suitability index in the central zone. However, as the MCE method is aimed to locate the best up-flow areas by making practical considerations to promote the location of successful drill sites, the explanation of the integral functioning of the geothermal system as a whole, main objective of the conceptual model, is not emphasized.

It is important to note that in some aspects data integration performed with the MCE is a more rigorous procedure that the solely intuitively-based data integration method, applied up to now by the CFE personnel to include the geothermal evidence in a conceptual models. Thus, if the procedure to calculate the suitability index to locate new drill sites is based on adequate interpretation criteria, their results can be used to modify our conceptual model of the field and should note be considered only as a method whose results must be adjusted by heart to the preexisting conceptual model. However, the use of a MCE method for a task other than the drill site location requires further study and is beyond the scope of this paper.

6.1 Criteria for specific drill sites selection from practical considerations

Once that a geothermal index was calculated for each cell based only on Earth Sciences data, the next problem to solve was to decide which cells among a set with similar values should be selected as a drill site. The geothermal index (Fig. 8 and 9) is just an aid to resume the importance of a set of geothermal data sources, but it lacks of real precision, so small numeric differences could be no-significant and must not be used with this aim.

We decided to group the raw geothermal index (Fig. 8) into three levels and consider that the best locations are those where the dominant contribution is owed to nearby superficial thermal activity and fault planes, especially those trending E-W. We justify this decision on the basis of results shown in Table 2 discussed in a previous section. In this way we give each recommended site a structural geology target with the aim of increasing the possibility of finding permeable intervals at reservoir depths where the borehole would be predicted to intersect the fault plane.

A GIS is a powerful tool to select the best drill sites on the basis of practical limitations of environmental, economic, social or political character. We tried incorporating some other layers that would reflect some of these concerns, but because of specific conditions at Los Azufres they did not provide useful results. We tried imposing, for example, a 500 m buffer from pre-existing roads, in order to avoid the proposal of sites requiring excessive opening of access roads; however, road density at Los Azufres is high and all of the best drilling prospects were inside the buffer. A 500 m buffer around fault planes was also attempted with similar unsatisfactory results. Anyway, these restrictions seem to be more valuable for selecting drilling locations in other less-developed geothermal fields.

Useful results were obtained by making a distance analysis of the new drill sites relative to pre-existing wells. With this aim we used a 250 m perimeter around previous successful wells as an exclusion zone for the location of new boreholes in order to avoid interference problems. Recent studies suggest that the area of influence could be around 180 m in some wells. In such a case for those locations a larger exclusion perimeter (twice this number or 360 m) could be a better selection.

The influence of injection wells in the reservoir was not considered for this study. Increasing in air-gases content of fluids discharged by wells to the west of the injection area has been observed, but the cooling effect has been negligible. A new study using tracers shows as preliminary results a complex flow pattern from the injection to the producing wells. All the injection wells (3, 7A, 8, 15, 52 and 61) are located in the limits of the best geothermal area and this boundary is well outlined by the geothermal index.

The proposed drill sites shown in figures 8 and 9 indicate the location of the drilling targets at depth because they were selected on the basis of the subsurface 3D-fault plane locations. On the other hand, experience with directional drilling with Mexican contractors show us that a 500 m of horizontal displacement is an upper limit that we have to consider in order to avoid excessive drilling risks and costs. That is the reason why we used a 500 m buffer around the drill sites to decide the locations on the topographic surface at which we can start drilling. In particular this let us determine if a preexisting drill-pad could be used to place the drill rig at the surface.

Table 4 presents the results of an algorithm to locate the nearest preexisting wellhead to each new drill site. Minimum distances to drilled wells smaller than 250 m, shown in the last column of Table 4, occur when the nearest drilled well to a proposed drill site is non-productive. The use of a 500 m buffer around the new drill sites showed that most of them can be reached from preexisting drill-pads so that investment and environmental concerns can be satisfactorily resolved. By means of the practical considerations described in the previous paragraphs we selected the drill sites indicated in figures 8 and 9.

6.2 Results validation

There are two related but distinct problems associated with the testing of the validity of MCE. The first one responds the question of how well the MCE method let us to emulate the conventional methods used by geologists to locate new drill sites, and the second responds the question of how successful in terms of total thermal discharge are the selected locations using the MCE. The first problem is related to the implementation of software and the procedure we present in this paper. With this aim we compare the drilling sites selected with the MCE method and those selected in an independent study by the field CFE personnel using the conventional methodology (included in figures 8 and 9) (Residencia de Los Azufres, 2003). We found a good agreement, and differences are related to differences in personal criteria not to the use of the MCE method, as is discussed in this section.

Proposed site name	X coordinate[a] [m]	Y coordinate [m]	Risk level[b]	Nearest drilled well	Horizontal distance to the nearest well [m][c]
x01	324,604	2,193,401	low	27	214
x02	325,967	2,193,394	low	53	80
x03	324,107	2,192,463	low	65D	325
x04	323,863	2,193,338	low	42	372
x05	324,470	2,192,085	low	30	278
x06	325,108	2,190,004	low	23	559
x07	325,124	2,189,357	low	12	78
x08	325,360	2,188,876	low	47	343
x09	326,448	2,188,285	low	34	334
x10	325,731	2,188,774	medium	47	134
x11	324,619	2,189,586	medium	23	387
x12	324,872	2,191,880	medium	30	428
x13	324,848	2,190,555	medium	23	660
x14	325,613	2,190,469	medium	25	531
x15	325,092	2,189,042	medium	12	306
x16	326,409	2,188,734	medium	62	322
x17	326,393	2,193,133	medium	29D	412
x18	325,108	2,193,401	medium	57	509
x19	324,123	2,192,069	medium	41	410
x20	325,226	2,190,516	medium	25	789
x21	322,877	2,193,417	high	52D	532
x22	322,380	2,193,378	high	40	427
x23	322,641	2,192,550	high	15	368
x24	324,832	2,193,796	high	27	293
x25	326,622	2,192,589	high	29D	221
x26	325,163	2,191,872	high	9	450
x27	323,610	2,191,667	high	54	382
x28	326,086	2,191,833	high	49	314
x29	324,627	2,187,867	high	16AD	413
x30	325,258	2,187,599	high	16D	436
x31	327,134	2,189,310	high	35	450
x32	325,337	2,189,720	high	1	460
x33	326,377	2,187,631	very high[d]	11	580
x34	326,362	2,189,885	very high	25	572
x35	326,377	2,191,123	very high	49	925
x36	323,610	2,191,123	very high	3	431
x37	327,860	2,189,349	very high	35	1164

[a] Coordinates correspond to the drill target at depth.
[b] Risk level of finding a non-productive site.
[c] Horizontal distance over 500 m may require building of new drilling-pads.
[d] Sites with a very high risk level are proposed for exploratory purposes.

Table 4. Coordinates of new drill sites (targets at depth) resulting from this study, and distance to pre-existing wells.

The second problem is related to the evaluation of the geothermal interpretation criteria used to locate wells from a more philosophical perspective, isolated from the operational procedure to apply these criteria with the aid of a computer. Although a comprehensive study on this topic is outside the aim of this paper, some initial results of this task were discussed in the previous section.

It is important to notice that in figures 8 and 9 the location of drilled wells (crosses) and those proposed by the field personnel (circles) indicate the wellhead position and the line in the directional wells represent the horizontal displacement at depth, while the drill sites proposed in this paper correspond to the target at production depth. There is a good agreement of well sites 47A, 23D and 74 (field's personnel nomenclature) with low risk sites proposed in our study. Wells 71 and 75 does not have a correspondence because they are located in the flanks of high suitability contours but their distance to several pre-existing wells is very near the minimum 250 m distance and consequently the size of the target area is small, so, we preferred to omit those sites. Borehole 70 is proposed to use a pre-existing drill-pad and its deviation tends to a high suitability anomaly in which we locate a high risk production well. Wells 68D and 73D are located near a low-risk site but the field personnel proposal selected a different fault as target at depth. Sites 08A and 07A are for injection wells, category that we did not include in our study. However, they are located in suitability contours that indicate the western limit of the known reservoir.

For this study we have not included subsurface data from directional wells due to lack of data and technical difficulties. That is the case in particular of the successful well 65D, located 30 m to the SE of the failed vertical well 44 (both in the same pad and overlapped by the drill site selected for the directional well 70 in figures 8 and 9). Directional data provided after the completion of this study indicate that well 65D has a horizontal displacement around 300 m to the SE. The success achieved by this well is compatible with the presence of a maximum of geothermal suitability index to the SE of well 70 in the same figure, where we located a low risk production site, indicated by a black square located a few meters away of the ending point of the 65D directional well. This result, yet of an inconclusive character, encourages the feeling that the geothermal index can be a useful indicator for the selection of new drilling sites.

We consider that the results of the MCE method are successful because of the agreement on several drill sites proposed by the two independent studies, and the fact that another drill sites proposed on the basis of traditional methods are compatible with the suitability contours that we have produced, in spite that we decided not to propose drill sites in those locations due to additional explicit considerations.

In this paper we considered that a high relative contribution of the layer containing fault planes to the geothermal index was an extra favorable evidence to support the location of a new drill site. Regardless this is a biased criterion it is easy to observe that the bias to field mapped faults and pre-existent productive wells is much more important in the proposal of drill sites by the Los Azufres personnel. In that case a preference to locate new boreholes in the middle of preexistent producing wells is noticeable. In that sense those more ‘conservative’ proposals can be considered of very low risk in relation with the location of high enthalpy fluids, but for the same reason the risk of interference with pre-existent wells is higher. If the inclusion of more data layers is a better procedure to locate drill sites or not is debatable, but a relevant fact is that using the MCE it is possible to find differences in data or hypothesis to explain discrepancies in the selected drill sites.

Due to the fact that in the MCE procedure the evaluation mesh corresponding to each geothermal variable is stored, it is possible to display them separately, to re-combine selected variables with a different relative weight or to restrict attention to geothermal data corresponding to a specific depth, for example. This flexibility is mandatory because at present we have not a way to demonstrate which should be the best integration criteria, and consequently each interpreter has his own personal opinion of which variables should be included and the relative weight for each one. In that case it suffices to repeat the weighted averaging process. However, if an interpreter requires modifying the criteria for the transformation of geothermal evidence to a numeric format, it is necessary to repeat also this part of the process for that layer to generate a new array’s column, but this can be done in an efficient way with the help of the user programs.

We used thermal discharge data to select the most meaningful variables, to assign them a relative weight, and to determine the geothermal meaning of data ranks of the variable for each specific method. Additionally, we used interpolated values of thermal discharge (and other variables measured in boreholes, like temperature and hydrothermal alteration) as predicted values in areas not drilled yet. In this way we systematically select new drill sites by a combination of drilling experience and exploratory studies (geology and geophysics).

When applying this procedure it is important to note that, as we are using interpolated values to calculate the geothermal index, it is advisable to ensure that the gridding calculation from irregularly distributed data is conducted with a careful application of geo-statistical methods, in order to ensure that the interpolated values be considered as true estimates of the variable.

In no way does the use of a MCE method intend that the decision making process for borehole location rely solely on a computer system. As noted earlier, it is strongly dependant on the experience and technical skills of geothermal researchers to decide the data layers included in the evaluation and the relative weight for each one. However, computer assistance is critical because visual comparison of maps and calculation of the geothermal index surpasses the human capability for these tasks.

In order to define a priority order for the 'low risk' drill sites, user software is prepared for the automated trace of geological-geophysical sections and 3D displays to make a detailed analysis of the subsurface geometry. Additional social or environmental concerns in plain view can be introduced as decision parameters by means of conventional GIS methods.

Results of new wells (whether these are selected or not using this MCE method) can be used to verify the correctness of assumptions and hypothesis accepted to calculate the geothermal index. With the verification of predicted results we will complete the application of a scientific method to locate new drill sites. In that way, even failed industrial results can be useful to increase our understanding of geothermal fields, and as a consequence increase the rate of successful to failed boreholes.

7. Conclusions

This project was feasible thanks to the comprehensive geothermal databases included in a GIS. Results can be divided in field-specific and methodological contributions.

The most important field-specific contribution is our proposal for new drill sites at the Los Azufres geothermal field, and the indication of their estimated relative risk. A distance analysis to study the influence of distance from production wells to surface thermal features and faults of different trends, gives quantitative support to conventional criteria used to select drill sites at that field.

The interpretation of topographic lineaments on DEMs suggests the existence of many N-S features not previously mapped. The identification of linear interfaces of Occam resistivity at different depths can be useful to locate hidden faults. These results show that the use of GIS and new digital maps in apparently well known areas, such as Los Azufres, is greatly rewarding, even when applied to studies usually recommended for the initial exploratory stage.

The drill sites selected in this study are compatible with those located using traditional methods, with the advantages of repeatability and explicitness in the use of variables and hypothesis discussed in the text. Discrepancies can be explained on the basis of the explicit criteria included in the MCE.

The evaluation of the success of the drill sites proposed in this paper, by comparing to the production results of the new wells drilled in the future, is a pending task less associated with the correctness of the MCE than with the correctness of the conventional interpretation criteria developed at Los Azufres for drill site location that we implemented with minor modifications.

The most important methodological contribution is the development of software and criteria for the use of a MCE method to evaluate simultaneously the best available geothermal data set to locate new production drill sites. Databases and software make possible to complete a new MCE in just a few hours, so, different evaluations can be conducted under different criteria and much more time can be devoted to research or interpretation.

The use of a MCE procedure has the intrinsic advantage to compel the interpreter to make an explicit evaluation of the criteria on which his interpretation relies. The use of explicit hypothesis and numerical procedures can be used to obtain repeatable results and, in this way, errors and misconceptions can be identified and corrected in future interpretations. We consider that using this MCE makes possible to do a faster, more rigorous, and better supported selection of new drill sites.

The assignment of weights is based on intuitive considerations but it is far from being arbitrary. However, advances in the statistical study on the contribution of different layers of geothermal evidence are necessary to diminish the subjectivity in the selection of weights.

The MCE method is adequate to give the geothermal exploration efforts in Mexico a more quantitative approach for map comparison, or to understand the success or failure of wells drilled in the past in light of the exploratory evidence used to locate them, and in this way to obtain a better understanding of the field and increase the ratio of successful to failed wells.

8. Acknowledgments

We thank Héctor Esquivias of the Residencia de Los Azufres for providing us with improved data on well locations, Reinaldo Waldo for well production data, and Santiago Rocha for the preliminary location of thermal springs. We are also indebted to Saúl Venegas and Jesús Arredondo of the Gerencia de Proyectos Geotermoeléctricos (CFE) for their interest and support for this study. Special thanks are due to Dr. Patrick Dobson and an anonymous reviewer whose comments were very useful to improve the original manuscript.

References

Bigurra P., E., 1995. Integración geofísica con sondeos eléctricos verticales en Los Azufres, Mich. Internal report No. GF-AZ-033/95, Gerencia de Proyectos Geotermoeléctricos, Comisión Federal de Electricidad, Morelia, México. Unpublished.

Coles, D., Y. Vichabian, R. Fleming, Ch. DesAutels, V. Briggs, P. Vermeesch, J.R. Arrell, L. Lisiecki, T. Kessler, H. Hooper, E. Jensen, J. Sogade, and F.D. Morgan, 2004. Spatial decision analysis of geothermal resource sites in the Qualibou Caldera, Santa Lucia, Lesser Antilles. *Geothermics* 33, pp. 277-308.

Davis, J.C., 1986. *Statistics and data analysis in geology*. Second Edition, John Wiley and Sons, New York, p. 7.

García E., G.H., 1995. Reinterpretación geofísica del campo de Los Azufres, Mich. (Reporte de avance). Internal report No. GF-AZ-034/95, Gerencia de Proyectos Geotermoeléctricos, Comisión Federal de Electricidad, Morelia, México. Unpublished.

García-Estrada, G.H., 2005. Integración de datos de sondeos electromagnéticos (TDEM) y sondeos eléctricos verticales (SEV) en Los Azufres, Mich., Internal report No. GF-Az-03-05, Gerencia de Proyectos Geotermoeléctricos, Comisión Federal de Electricidad, Morelia, México. Unpublished.

García-Estrada, G.H., A. López-Hernández, and R.M. Prol-Ledesma, 2001. Temperature-depth relationship based on log data from the Los Azufres geothermal field, Mexico. *Geothermics*, Vol. 30, pp. 111-132.

García-Estrada, G.H., and A. López-Hernández, 2003. The use of a GIS for the study of Geothermal fields-Results at Los Azufres, Mexico. Geothermal Resources Council *Transactions*, Vol. 27, pp. 609-613.

Huitrón E., R., O. Palma, H. Mendoza, C. Sánchez, A. Razo, F. Arellano, L.C.A. Gutiérrez N., and J.L. Quijano, 1991. Los Azufres geothermal field, Michoacan. In: Salas, G.P. (Ed.), *Economic Geology, Mexico*, Geological Society of America, The Geology of North America, Vol. P-3, pp. 59-76.

López H., A., 1991a. Análisis estructural del campo geotérmico de Los Azufres, Mich. Interpretación de datos superficiales y de subsuelo. Internal report No. 11/91, Gerencia de Proyectos Geotermoeléctricos, Comisión Federal de Electricidad, Morelia, México. Unpublished.

López H., A., 1991b. Geología de Los Azufres. *Geotermia*, Vol. 7, No. 3, pp. 265-275.

López-Hernández, A., G. García-Estrada y R. Hernández-Zuñiga, 1981. Implementación de un método geoestadístico como parte de la evaluación preliminar en zonas de interés geotérmico. Internal report No. 41-81, Gerencia de Proyectos Geotermoeléctricos, Comisión Federal de Electricidad, Morelia, México. Unpublished.

Marshak, S., and G. Mitra, 1988. *Basic methods of structural geology*. Prentice Hall, New Jersey, pp. 81-82.

Palma G., S.H., 2003. Comentarios sobre las propuestas de perforación en el campo geotérmico de Los Azufres, Mich. Internal report No. GF0309, Gerencia de Proyectos Geotermoeléctricos, Comisión Federal de Electricidad, Morelia, México. Unpublished.

Prol-Ledesma, R.M., 2000. Evaluation of the reconnaissance results in geothermal exploration using GIS. *Geothermics*, Vol. 29, pp. 83-103.

Residencia de Los Azufres, 1996. Información general del campo Los Azufres hasta 1996. Internal report in CD-ROM, Gerencia de Proyectos Geotermoeléctricos, Comisión Federal de Electricidad, Morelia, México. Unpublished.

Residencia de Los Azufres, 2003. Propuesta de construcción de pozos productores e inyectores para contar con vapor de respaldo y capacidad de inyección en el campo de Los Azufres. Internal report No. RAZ-RE-02/2003, Gerencia de Proyectos Geotermoeléctricos, Comisión federal de Electricidad, Morelia, México. Unpublished.

Saaty, T.L., 1977. A scaling method for priorities in hierarchical structures. *J. Math. Psychology*, 15, pp. 234-281.

Tello H., E., 1997. Geochemical model update of the Los Azufres, México, geothermal reservoir. Geothermal Resources Council *Transactions*, Vol. 21, pp. 441-448.

Tello H., E., 2005. Estado de equilibrio soluto-mineral y saturación de minerales de alteración en fluidos geotérmicos de alta temperatura de México. Ph.D. Thesis, Facultad de Ingeniería, Universidad Nacional Autónoma de México (UNAM). Unpublished.